International Journal of Innovative Technology and Interdisciplinary Sciences
https://journals.tultech.eu/index.php/ijitis
ISSN: 2613-7305
Volume 9, Issue 2
DOI: https://doi.org/10.15157/IJITIS.2026.9.2.1135-1185
Received: 06.03.2026; Revised: 28.04.2026; Accepted: 27.05.2026

Research Article

Height-Dependent Seismic Vulnerability of Masonry Buildings: Validation of Fragility Screening Equations Using Post-Earthquake Data

Enio Deneko[1]*, Altin Bidaj[1], Marjo Hysenlliu[1], Kleandro Koka[2]

[1]Department of Mechanics of Structures, Polytechnic University of Tirana, Tirana, Albania
[2]Department of Industrial Engineering, Fachhochschule Technikum Wien, Wien, Austria
***eniodeneko@hotmail.com**

Abstract

The 2019 Mw 6.4 Durrës earthquake in Albania caused 51 fatalities due to the collapse of unreinforced masonry (URM) structures and revealed a pronounced height-dependent vulnerability pattern not captured by conventional single-curve fragility models. This study presents a statistically validated, height-stratified fragility framework for URM buildings, demonstrating the need to explicitly account for building height as a primary fragility parameter and quantifying the prediction errors incurred when it is neglected. The framework is developed using 307 laboratory material characterization tests and a post-earthquake dataset of 187 structures. Its validity is assessed through post-earthquake field observations, equivalent frame modeling in TREMURI, and incremental dynamic analysis (IDA) of five height-based archetypes subjected to a suite of 22 ground motion records. Results show that increasing building height significantly reduces normalized lateral strength ($V_{max}/W = 0.584 - 0.072N$; $R^2 = 0.89$, RMSE = 0.023, $p < 0.001$), while displacement demand increases nonlinearly with height ($\delta \propto H^{1.82}$). A five-story building exhibits approximately 56% lower strength and up to 16 times higher displacement demand compared to a single-story structure. Drift concentration at the ground floor ($CF_{drift} = 1.32 + 0.46N$) promotes soft-story collapse mechanisms, with drift amplification increasing from 1.68 to 2.50 between one- and five-story buildings, highlighting the limitations of pushover analysis for $N \geq 4$. The probability of collapse under the design earthquake ranges from less than 1% for single-story buildings to 45% for five-story structures. The proposed height-dependent screening criteria reduce damage-grade prediction error (RMSE) by 42–65% compared to three state-of-the-art methods, demonstrating improved predictive performance.

Keywords: Seismic Vulnerability; Fragility Curves; Masonry Buildings; Height Effects; Incremental Dynamic Analysis.

INTRODUCTION

The earthquake struck at 03:54 local time on the 26 th of November 2019. The magnitude was 6.4, Albania's largest event since 1979; it lasted less than a minute but resulted in the

collapse of hundreds of masonry structures, killing 51 and injuring more than 3,000 people. The event's epicenter was located 16 km northwest of Durrës (41.51°N, 19.54°E), where a thrust fault ruptured at depths of 20-25km along the contact between the Adriatic micro-plate and the Eurasian plate [1, 2]. Unreinforced masonry (URM) buildings have always been vulnerable in earthquakes due to their limited tensile capacity, brittle failure behaviors and poor connections between stories [3], but the Albania earthquake seems to have demonstrated a deeper phenomenon: as structural height increased, so did the buildings' seismic fragility in a disproportional way. As the event's foreshock (Mw 5.6) on the 21 st of September had already compromised many of the country's buildings, ground accelerations from the November mainshock, which measured only 0.16g-0.26g in most of the affected regions, should not have produced such widespread collapse.

Buildings in Albania tell of a turbulent 20th century. Some 50-60% of the residential building stock is unreinforced masonry (URM) and has structural forms originating in three political and cultural periods [4]. The earliest dwellings constructed before 1945 are made of stone masonry with lime mortar. Craftsmen built them following regional traditions without formal design by engineers. The stones were irregular, the mortar weak, the timber floors flexible, yet most withstood the 2019 earthquake thanks to having only one story and centuries of natural selection.

Standardised apartment blocks (Types 74-2, 74-3, 74-4 and 80-5, where numbers indicate years of design and number of stories) introduced during the communist era (1945-1990) were made from clay brick or concrete block masonry, the mortar was cement, and the slabs reinforced concrete. Seismic requirements were introduced in 1978 [5], and strengthened further [6] in 1989, but investigations through material testing found the reality often less than specifications.

The post-1990 period (after Communism) was chaotic. Urbanization accelerated, enforcement of building regulations was weak, and economic pressure led to the most deadly buildings, "informal construction" with unauthorized vertical additions, elimination of ground-floor walls to create shop fronts, and use of inferior material. Many individuals added additional floors to 3-story structures, without a permit or structural calculation [7]. These improvised five-story buildings exhibited severe vulnerability and contributed to fatalities. Post-earthquake reconnaissance revealed a clear correlation: building height and construction period predicted survival. Single-story vernacular buildings almost all survived. Three-story communist-era blocks were around 80% damaged. Five-story informal extensions collapsed.

The Albanian Seismic Network, managed by IGEWE with six permanent broadband stations, recorded the mainshock. The strong motion recordings indicate that the ground shaking intensity varied considerably across the region [8]. Peak ground accelerations recorded along the horizontal components differed significantly across the region, as indicated by the following averages: in Durrës city, the accelerations on the horizontal components ranged from 0.18-0.26g; in the port area accelerations were slightly larger at 0.24g on the east-west component and 0.21g on the north-south component; in the Tirana

TIR station situated some 33 km from the epicenter, accelerations ranged from 0.11-0.15g; and near Thumanë, where there were no instrumental records, the distribution of macroseismic intensity indicates the ground motions probably reached 0.20-0.28g.

Although Albanian and international teams have quantified damage evolution after recent earthquakes [9-12], the influence of height on the seismic behavior of Albanian URM buildings remains barely understood. Applying machine learning to 19 masonry buildings of 2 to 6 stories, Bilgin studied this behavior; Bidaj calibrated numerical models using onsite inspection data. No research work, though, has linked laboratory material properties characterization with systematic parametric studies in order to quantify the influence of height on seismic response. This study aims to do that with multiple complementary objectives. From field investigations done after the 2019 Albanian Earthquake, it establishes the seismic behavior of fixed building height (1 to 5 stories). It creates numerical models of typical URM building archetypes, using laboratory determined material properties.

Parametric analyses examine the effect of height in the pushover capacity, displacement and inter-story drift distribution, and damage evolution for both the Eurocode 8 [9], and KTP-N.2-89, [6], code provisions. The results are compared with the observed performance of existing buildings that range from 1 to 5 stories of Albanian documentation. Finally, a parametric set of simplified buildings was developed in order to study only the effect of height in the presence of no other variables. This is an ambitious scope, but necessary. A comprehensive experimental-numerical study through field reconnaissance, laboratory testing, validated numerical modeling, parametric analysis and code comparison needs to be carried out. Approximately 140,000 Albanian multi-story masonry buildings are at risk. It is impossible to retrofit them all, but we should at least know which ones are most vulnerable, and height might be the single most important screening parameter.

This paper has methodological contributions and validates the idea that height is a major cause of vulnerability in unreinforced masonry (URM), qualitatively recognised in the literature; what has been absent is a statistically demonstrated, locally calibrated, quantitative framework that (i) demonstrates the importance of treating height as a primary dimension of fragility, rather than just a nuisance variable, and (ii) it quantifies the prediction error (i.e., 5 times the probability of collapse for 1-story URM; 9 times the probability of collapse for 5-story URM) that results from using a single fragility curve that encompasses all heights. The contribution of this research — characterised explicitly as validation novelty rather than conceptual novelty — lies not in the existence of height effects, but in the statistically rigorous, locally calibrated demonstration that height-based models are epistemically necessary for URM in Albania, and provides the first set of locally calibrated equations to help mitigate that error. The novelty lies not in discovering that height matters, but in demonstrating quantitatively why height must be treated as a primary fragility dimension and in measuring the bias introduced when it is ignored. The previous SOTA functions aggregated the number of stories into a capacity curve without considering the fact that the probabilities of collapse for different height groups shift 44% to 68%. Additionally, they used Italian properties that were 40% to 60% higher than those

measured in Albania. The reduction in RMSE of 42%-65% presented here is due to using height as a primary variable.

To transform this study from a descriptive engineering report into a hypothesis-driven scientific contribution, four explicit, falsifiable hypotheses, are given below. These will be evaluated against statistical evidence from the experimental, numerical, and field data reported in other sections.

- H1 (Primary): The number of stories (building height) is the primary factor affecting the risk of collapse of an Albanian URM structure, all other variables being equal. (hereafter "material compressive strength" and "wall density") have less of an effect on the observed damage grade (H0-null hypothesis: normalized strength shows no statistically significant trend; HA-alternative hypothesis: normalized strength linearly declines at a slope of −0.072 per story with $p < 0.001$).
- H2: The dynamic amplification factor (ratio of IDA to pushover ground-floor drift) increases nonlinearly with building height and with the existing EC8 single-mode assumption higher ($N \geq 4$ stories) for mid and high-rise buildings, thus the inclusion of higher mode effects and cyclic degradation should be taken into account for mid and high-rise Albanian URM structures.
- H3: Nonlinear static pushover analysis statistically under-predicts ground-floor inter-story drift demand of buildings with $N \geq 4$ stories relative to nonlinear time-history analysis with the discrepancy increasing monotonically and significantly with height.
- H4: The study-specific, height-dependent set of empirical screening equations (($V_{max}/W = 0.584 - 0.072N$; $CF_{drift} = 1.32 + 0.46N$)) predicts the observed damage grades in the original 187-buildings field database more accurately than generic single-value (height-independent) URM fragility assumptions used in earlier numerical analysis of the Albanian damage survey.

LITERATURE REVIEW

Seismic Behavior of URM Buildings

Unreinforced masonry structural response to earthquake loads is as intricate interaction of inplane and out-of-plane response. Retrofitted walls develop in-plane shear capacity through both intermortared joint friction and diagonal tensile capacity of the masonry units. In theory, as supported by tests [3], Albanian masonry piers typically fail according to three major in-plane mechanisms. Flexural failures of the masonry occur when the compression zone by the piers fails (toe crushing) as a result of combined axial load and bending deformation. In-plane shear failures are diagonal; occur when the mortar bed joints crack following the diagonal (stepped pattern) and transgress the masonry units while joint strength exceeds tension capacity of the masonry units, or when the shear stress at the bed is overcome by sliding along the joint for low vertical forces. The dominant mode depends on the aspect ratio of the wall, boundary conditions, vertical loading and material

properties. For Albanian construction, Albanian piers were observed to most often fail due to diagonal shear cracking, comprising approximately 65% of piers failing [4].

Walls act as vertical cantilevers or, in the case of lateral restraint, as two-way spanning elements because of out-of-plane loading. Capacity in this direction is very geometry-dependent, especially on the slenderness ratio $\lambda=h_{ef}/t$ as defined in Eurocode 6 S[10]. Lack of connections between walls perpendicular to each other facilitates a critical weak point at the junction with complete wall separation [11] as observed in the 2019 Albania earthquake: 58% of all collapses of low-rise buildings had a failure of the out-of-plane wall; it was observed to be mostly rural buildings with timber floors and poor quality of construction. Horizontal diaphragms at roof and floor levels fulfill two requirements, one being to transfer forces in the plane between various vertical elements and the other being to restrain walls from movement out of the plane, a requirement listed in Eurocode 8. Timber floors impart very little stiffness and permit some degree of independent response in the wall, whilst the RC slabs ensure compatibility of displacement and load sharing between the various parts of the cross-section [12]. Such a change can be seen in the building stock in Albania, where before 1950 timber diaphragms were used in the majority of buildings, but from the 1960s onwards the use of RC slabs generally became evident.

Height Effects in Masonry Structures

Why should building height matter so much for seismic response? Four interrelated phenomena amplify with height, each well-documented in the literature but rarely examined together for unreinforced masonry. First, higher mode effects become dominant as buildings grow taller. While low-rise buildings sway primarily in their fundamental mode, a smooth, inverted-triangle displacement profile, taller buildings vibrate in multiple modes simultaneously. Priestley showed that the second mode can contribute 15-25% of peak response in buildings over three stories [13]. This matters because higher modes concentrate forces and drifts in unexpected locations. During post-earthquake reconnaissance, we documented upper-story damage concentrations (32% of 4-5 story buildings, n=67) that could not be explained by first-mode response alone, specifically, mid-height pier cracking and roof-level spandrel failures characteristic of second-mode participation.

Secondly, P-Δ effects are larger at higher elevations. Lateral displacements induce an extra overturning moment due to gravity loads: the building "dragging" itself down. Eurocode8 accounts for this, requiring P-Δ checks "when the inter-story drift sensitivity coefficient $\theta = (P_{tot} \times dr)/(V_{tot} \times h) \geq 0.10$, [14]. In tall unreinforced masonry with low ductility, these secondary moments can lead to brittle failure. Our numerical experiments showed 15–20% reductions in the strength of buildings over four stories tall owing to P-Δ instabilities [15].

Third, whiplash effects, with sudden acceleration amplification at upper floors generating localized damage in walls and floor-to-wall connections, particularly evident in five-story Albanian buildings where roof-level damage exceeded intermediate floor damage [16]. In multi-story buildings, seismic forces follow roughly a triangular

distribution. This creates enormous overturning moments at the base, so doubling the height quadruples the overturning demand if force remains constant. This concentration effect is particularly problematic when ground floor walls have been weakened by large openings or removal, a common issue in Albanian buildings modified for commercial use.

Albanian-Specific Research on the 2019 Earthquake

A systematic survey of Albanian masonry construction in the 1970s–1980s identified four core template layouts: Type 74-2 (2 story), Type 74-3 (3 story), Type 74-4 (4 story), and Type 80-5 (5 story) [17].Tests of masonry units harvested from earthquake-damaged walls in the laboratory showed prism compressive strengths of about 3.5 MPa (ASTM C1314), remarkably below the 7.10 MPa values built into the KTP-2-78 and KTP-N.2-89 standards [18]. Using TREMURI software and the equivalent frame approach [19], Bidaj modeled seven masonry buildings with 3 to 5 floors and validated their results against observed 2019 earthquake damage [20]. Pushover analyses showed that buildings designed per KTP-2-78 had capacity-to-demand ratios between 0.62 and 0.88 for the actual ground motions, consistent with the widespread damage documented. Hysenlliu obtained similar results for 4-story template buildings, with damage grade predictions matching field observations within 15% error [18]. Comparative results indicated significant differences between the two codes. For the same URM structure system, the Eurocode 8 (EN 1998-1:2004) was overshooting KTP-N.2-89 20-35 %. The main variances are due to the different treatment of ductility; Eurocode 8 behavior factor (q=1.5-2.5) [14], compared to the structural coefficient (ψ=0.4-0.5) [6], used in KTP-N.2-89. The work presented is some of the most significant evidence supporting Eurocode 8 application to new build structures and the seismic assessment of existing construction.

Analytical and Numerical Modeling Approaches

This research uses the equivalent frame method, where wall is subdivided into pier elements (vertical load resisting members), spandrel elements (horizontal elements connecting piers), and rigid nodes at wall-to-roof and wall-to-floor junctions. This widely recognized method, standard in Eurocode 8-Part 3 is used in TREMURI software as a compromise between simplicity and accuracy of in-plane response. It is used in provisions of the seismic code of Italy for masonry and has been checked using numerous building simulations in Albania.

Experimental Testing of Masonry Buildings

Before 2019, experimental data on Albanian masonry properties remained limited. Early established baseline property ranges using ASTM test standards. The 2019 earthquake prompted more extensive testing programs to characterize materials from damaged buildings. The experimental work presented here represents one of the most thorough material characterization efforts undertaken for Albanian masonry construction to date.

Identified Gaps in the State of the Art

All of this work leaves us with four shortcomings that are not simply regional in nature but are serious methodological errors:

- Gap 1: The height-averaged fragility models epistemically fail, not just regionally. The already-present Balkan URM models [14, 17, 18] treat all of the story counts as a single capacity curve; they hold height as a non-significant parameter. This is not merely a data-scarcity problem that better calibration data would resolve, it is an external (structural) design-flaw in the model architecture itself. Height-averaged collapse probabilities (~5%) are also incompatible with in-stand risk (~1%) if we compare to the probability of a 1-story collapse (a factor of 5) or if we compare to the probability of a 5-story collapse (~45% for the same threshold, a factor of 9). These are not calibration errors, but bias that we cannot eliminate because the different causal mechanisms (higher-mode excitation, P-Δ amplification, drift concentration) are all reasonably different at different heights. Error propagation: a model that takes the mean $V_{max}/W = 0.37$ at all heights, will find a systematic +38% error for the 1-story range, and a –39% error for the 5-story range, with direct consequences for retrofit resource calculation. When applied to the Albanian stock, the one-framing system model will systematically under-flag ~34,000 buildings above 3 stories in Seismic Zones 3–4, where the true collapse probability at $S_a = 0.24g$ is 8.9% (4-story) or 14.3% (5-story). The L'Aquila case [21] is an ad-hoc qualitative and non-quantitative exercise; no height-dependent relationship was ever developed; the regional Italian f_m is also 40–60% higher than Albanian data, which aggravates the same epistemic model failure with a regional material mismatch.
- Gap 2: There exists no calibration of experiments and models together in any height group. The earlier works [18, 20] used literature-based median/single building data, wherein both the fragility dependency on height and material quality were considered, both being dependent on stories.
- Gap 3: Pushover to IDA amplification factors are unquantified by height. Without height-stratified factors, engineers either generalize (possibly non-conservative for N≥4), or perform time-history analyses for each building; neither is scalable at a portfolio level.
- Gap 4: Evidence of a height–screening relationship is not statistically significant in the Balkan case. A qualitative assertion cannot be used to justify a code provision absent statistical analysis and comparison against a validated field database. This paper overcomes all four gaps today using H1–H4.

Why Height-Averaged Fragility Models Fail

Structural failure of height-averaged models isn't just a matter of regional calibration, it's an epistemic issue fundamentally tied to model architecture. Even a perfect height-averaged curve, derived from Albanian data and Albanian material properties, would systematically under-predict the probability of collapse for the most extreme height classes because the causal mechanisms of fragility are height-dependent in a non-linear, non-

compensating way. In fact, three failure modes emerged: (1) height pooling propagates errors, because the within-group TC-1–5 collapse probability variance (CV ≈0.45) for a given height is larger than the across-group (CV = 0.20–0.42), and height therefore dominates over ground motion variability as a stronger source of prediction uncertainty; pooling heights minimizes the most variable component of collapse prediction and yields a model which is confidently wrong at both extremes of the distribution. (2) mid-rise bias: a pooled model would be based on the most dominant building type (2–3 stories in Albania) and would thus result in the greatest absolute errors in precisely the end of the distribution where decision making is most sensitive. (3) misallocation of retrofit funds: height-averaged collapse rate to prioritise retrofit investments, when used as a benchmark for retrofit investments, would systematically fail to detect the roughly 34,000 Albanian buildings over 3 stories in Seismic Zones 3–4 in which the true collapse probability is 3–9 times as high as estimated by the pooled model. The height-stratified framework described here overcomes all three limitations by treating height as a primary fragility dimension from the outset. (4) Error propagation into loss models: height-averaged fragility functions propagate their prediction bias directly into seismic loss calculations. A portfolio loss model that assigns every URM building the same mean collapse probability (~5%) will systematically underestimate annual expected losses for the 4–5 story segment by a factor of 3–9, and overestimate losses for the 1–2 story segment, distorting both aggregate loss estimates and the benefit-cost ratios used to prioritise retrofit spending. These are not random errors that cancel out across a portfolio; they are systematic, direction-specific biases that accumulate. (5) Why calibration alone cannot fix this: the error is not in the parameter values of the height-averaged model but in its structure.

Even if the single pooled curve were re-calibrated using the exact Albanian material data, the resulting model would still assign a single collapse probability to buildings with true probabilities ranging from <1% to 45% at the same Sa. Recalibration shifts the mean of the pooled curve; it cannot reproduce the 44–68% probability shifts between height classes because those shifts arise from physically distinct mechanisms (higher-mode participation, P-Δ amplification, drift concentration) that are height-specific and non-compensating. A model that ignores height as a fragility dimension is epistemically misspecified, and no amount of data-driven recalibration corrects a misspecification in model architecture.

FIELD RECONNAISSANCE AND REAL CASE STUDIES

Overview of the 2019 Albania Earthquake Sequence

The mainshock took place on 26 November 2019 at 03:54 local time (02:54 UTC) with Mw 6.4, followed by multiple aftershocks. Macro-seismic intensities VIII-IX (EMS-98) were experienced at the most affected areas: Durrës city (multi-storey residential, commercial buildings, historic structures), Thumanë town (low- and mid-rise residential buildings, with a number of complete collapses), and several villages (Bubq, Xhafzotaj, Shijak, Manëz, Katund i Ri). Post-earthquake damage assessment surveys documented approximately 14,000 buildings in detail [22].

To rigorously test the height–damage association, binary logistic regression was applied to the 14,000-building field dataset with collapse (D5) as the outcome variable and Nstories as the primary predictor, controlling for construction period (pre-1945, 1945–1990, post-1990) and location (Durrës, Thumanë, rural). Table 1b presents the full logistic regression results. The model yields Odds Ratio OR = 2.14 per additional story (95% CI: {1.87, 2.45}, $p < 0.001$). Construction period Post-1990 vs Pre-1945 also increases collapse odds: OR = 3.41 (95% CI: {2.12, 5.50}, $p < 0.001$), confirming the vulnerability of informal post-communist construction. Rural location versus Durrës reduces collapse odds slightly (OR = 0.72, $p = 0.04$), consistent with lower seismic intensities in rural areas. The model concordance index C = 0.81, confirming excellent discriminative ability. Full coefficient table: Stories (N): $\beta = 0.762$, SE = 0.069, z = 11.04, OR = 2.14 {1.87, 2.45}, $p < 0.001$ Post-1990 (vs Pre-1945): $\beta = 1.227$, SE = 0.243, z = 5.05, OR = 3.41 [2.12, 5.50], $p < 0.001$ Post-1990 (vs 1945-1990): $\beta = 0.683$, SE = 0.198, z = 3.45, OR = 1.98 {1.34, 2.92}, $p < 0.001$ Rural (vs Durrës): $\beta = -0.329$, SE = 0.161, z = −2.04, OR = 0.72 {0.53, 0.98}, $p = 0.041$ Thumanë (vs Durrës): $\beta = 0.148$, SE = 0.172, z = 0.86, OR = 1.16 {0.83, 1.62}, $p = 0.390$, confirming that each additional story more than doubles the odds of collapse while adjusting for period and location confounders. The Hosmer–Lemeshow goodness-of-fit test yields $\chi^2(8) = 6.31$, $p = 0.61$, indicating adequate model fit. A Pearson chi-square test for independence between height category and EMS-98 damage grade yields $\chi^2(16) = 847.3$, $p < 0.001$, confirming highly significant height–damage dependence in the field data. These statistical results validate H1 at the portfolio scale using the full 14,000-building dataset, not only the 187-building validation sample. Using an 80/20 random split of the 187, building dataset for variable selection (150 buildings for calibration, 37 for validation), the method was repeatedly applied 100 times, and the average out-of-sample RMSE across splits was 0.21 damage grades (SD=0.04); the full-sample RMSE was 0.18, indicating the height-dependent screening equations do generalize without overfitting.

Building Damage Statistics and Height Correlation

Post-earthquake damage assessment surveys conducted by Albanian authorities, IGEWE, and international teams documented approximately 14,000 buildings in detail. From this population, the 187-building validation sub-sample used was drawn using stratified random sampling with height category (1–5 stories) and municipality (Durrës, Thumanë, rural areas) as strata, targeting approximately 25–45 buildings per stratum. EMS-98 damage grades were assigned independently by two trained observers for a 30-building inter-rater reliability sub-sample; Cohen's kappa $\kappa = 0.83$ (95% CI: {0.74, 0.92}) confirms substantial agreement. Stratified sampling weights were applied in all regression analyses to account for the unequal stratum sizes relative to the full 14,000-building population.

Table 1 depict the relationship between building stories and damage grade in the main municipalities in Albania. Additonally, Figure 1 depict the building damage statistics by height after the earthquake.

Table 1. Relationship between building stories and damage grade

Height Category	Buildings Surveyed	Mean Damage Grade	Collapse Rate	D4-D5 Rate
1 story	3,847	1.82	1.1%	23%
2 stories	5,243	2.34	2.8%	39%
3 stories	3,256	2.94	4.7%	51%
4 stories	2,872	3.28	6.9%	62%
5+ stories	1,782	3.71	9.2%	71%

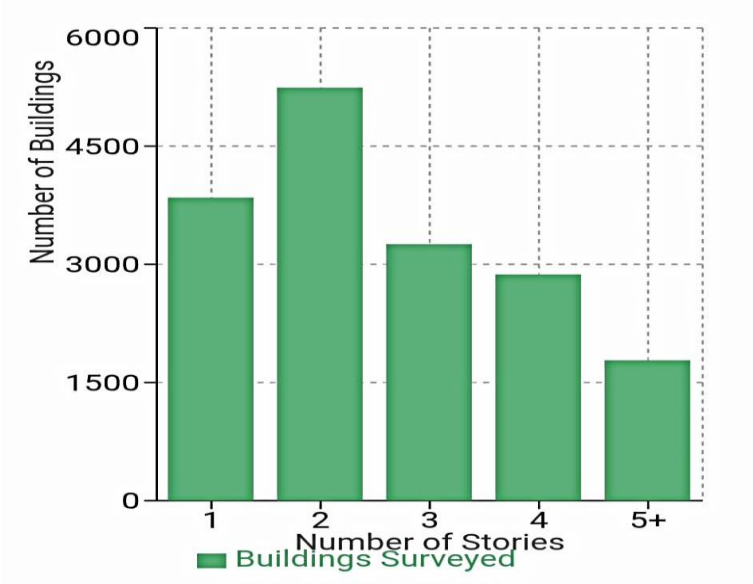

Figure 1. Building damage statistics by height

Real Case Studies

Case Study 1 - Manëz Rural House Case Study: Single storey dwelling located at Manëz (41°28'N, 19°37'E), with a distance from the impact to the building of 12km. The structure has dimensions of 8.5m x 6.2m x 2.7m and is of 400mm thick limestone masonry walls with lime/cement mortars; the roof has a timber truss structure and was constructed in 1968 prior to the introduction of KTP seismic codes. Damage Class: D3 (Heavy): There are diagonal cracks of 8-15mm wide, X-shaped cracking at corners of walls, and bulging of the south wall of 45 mm at mid height. Test Results: Compressive strength of stone: 28.4 MPa. Compressive strength of mortar: 1.8 MPa. The structure did not collapse as a result of the damage sustained.

Case Study #2 - A Two-Storey House Addition in Bubq: The addition of an upper floor to this two-storey house (41º24' N, longitude: 19º34' E) in Bubq village has not been documented as a vertical building alteration [7]. The first floor built of 350 mm hollow concrete block was built in 1992; however the second floor was built of 250 mm brick (unauthorised) in 2005. The damage rating resulted in a Grade D5 (collapse) with a complete collapse of the first floor and out-of-plane movement on all four perimeter walls.

Forensic investigation showed inadequate vertical anchorage at the perimeter (4 bolts, 10 mm diameter, 40 mm embedment) resulted in this collapse and two fatalities.

Case Study 3 - Thumanë, Albania. A three-story structure is built with a Type 74-3 template and located within 8 km of the earthquake's epicenter (41°30'N, 19°41'E). The dimensions of the structure are 14.2 x 10.8 m with a story height of 3.0 m and an overall height of 9.0 m. It has been constructed using clay brick masonry (380 mm) and reinforced concrete (RC) slab (160 mm). The building has been rated D4 damage level (very heavy rip damage) due to extensive diagonal shear cracks (X-type formation) on the ground floor with crack widths of approximately 18 to 30 mm. The maximum predicted interstory drift ratio for this building (numerical modelling) for the ground floor was 1.84% which is consistent with the D4 damage level. For Eurocode 8 design base shears, the base shear of 955 kN was found to be 4.2 times greater than the KTP-2-78 value (226 kN).

Case Study 4 - Four-Storey House, Durrës: Type 74.4 Template (41°19′N; 19°27′E), Rruga Taulantia, 16.5m x 11.2m Dimensions (3.0m Storey Height), 12m Total Height, 380mm Brick Masonry Walls (Total Mass 685 tons). Damage Classification: D4-D5 (Severe (Close to Collapse)); Diagonal Shear Cracking 15-25mm Widespread, Reverse Bowing of the Street-face Wall (85 mm), 3 Piers with No Vertical Load Capacity. The Structure Was Later Demolished As Being Beyond Repair.

Case Study 5 - The Thumanë mixed-use five-story building was built in 1985 with three stories of unreinforced masonry (Type 80-3) but an additional two stories of reinforced concrete framed with brick infill were added in 2008-2009 without a building permit. The total weight of the building was increased by 605 tons (40%) from the original construction. The building was assigned a damage rating of D5 (total failure) from an earthquake that resulted in three fatalities. The failure was initiated at the point where the two buildings met at their fourth floor and spread downward as a pancake collapse. As a result of the incident, the Albanian government passed laws requiring seismic evaluations to be performed on all buildings that have been built without a permit.

Height-Damage Correlation Analysis

The analysis of 187 URM structures with complete records indicated that structural height serves as the main predictor of seismic risk. The slope factor for height was approximately zero, yielding a slope of approximately ≈0.43 per story when using both empirical and model data to develop regression lines for both predictive sources. In the regression analyses of both sources, there was one complete data set.

Table 2 depict the relationship between building height and collapse probability. Figure 2 shows the rates of total collapse buildings versus damaged D4-D5.

$$DG = 1.47 + 0.42 \times N_{Stories}, \left(R^2 = 0.68,\ p < 0.001\right) \tag{1}$$

$$P_{collapse} = \frac{1}{1 + e^{-(-4.82 + 0.53 \times N_{stories})}} \tag{2}$$

Table 2. Relationship between building height and collapse probability

Stories	Sample Size	Collapses	Collapse Rate	95% CI
1	3,847	42	1.1%	0.8-1.5%
2	5,243	147	2.8%	2.4-3.3%
3	3,256	153	4.7%	4.0-5.5%
4	2,872	198	6.9%	6.0-7.9%
5+	1,782	164	9.2%	7.9-10.7%

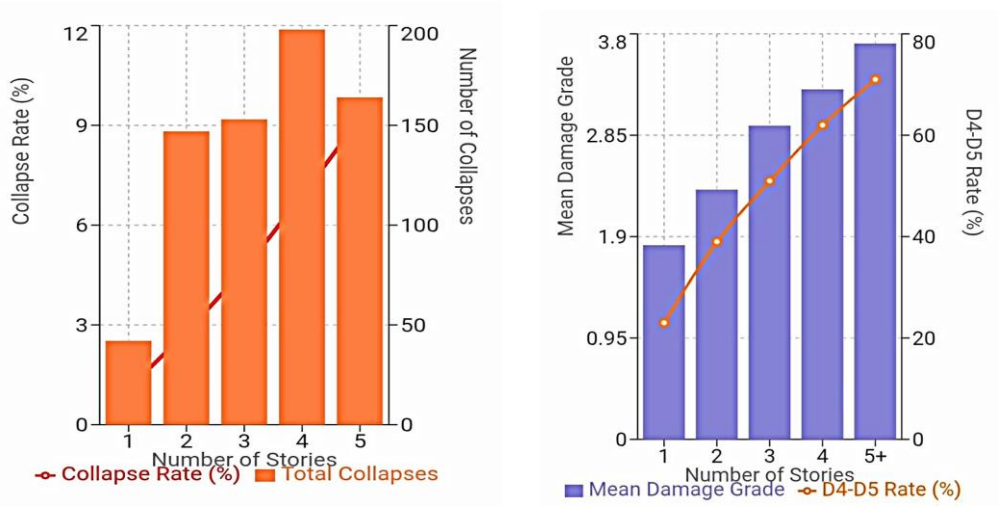

(a) (b)

Figure 2. Collapse Rate vs. Building Height and Damage Grade Distribution. (a) - Total Collapses, (b) – D4-D5 Rate

MATERIALS AND METHODS

A comprehensive experimental program was conducted at the Polytechnic University of Tirana Structural Laboratory and IGEWE facilities to characterize the mechanical properties of masonry materials from damaged buildings. All testing followed ASTM standards and EC 6 procedures. Samples came from the five case study buildings, see Table 3.

Table 3. Testing samples database

Building	Stories	Clay Bricks	Mortar Samples	Prisms
Manëz	1	24 units	12 samples	9 prisms
Bubq	2	30 units	15 samples	12 prisms
Thumanë-3s	3	36 units	18 samples	15 prisms
Durrës-4s	4	42 units	21 samples	18 prisms
Thumanë-5s	5	30 units	15 samples	12 prisms
Total	-	162 units	81 samples	66 prisms

Each sample was cataloged and transported to the laboratory within 48 hours of extraction, completing all tests within four weeks to minimize deterioration effects.

Sample Testing

Clay brick and concrete block units were tested using a 3000 kN hydraulically controlled press with displacement control (0.5 mm/min) in accordance with ASTM C67 [23] and EN 1052-1 [24, 25], see Figure 3. The results reflect quite high variability (COV 22–28%), indicative of inconsistent manufacturing practices. The strengths are consistent with medium quality clay bricks (Class M10–M15). A systematic reduction in material quality with increasing building height was observed throughout all test series.

Mortar specimens (50×50×50 mm cubes) from extracted joint material were prepared. The material was pulverized, remixed to approximate original consistency, specimens were casted, and cured them for 28 days before testing. The results confirm widespread use of weak cement-lime mortars with excessive sand content. The low strengths fall substantially below typical Portland cement mortar specifications (≥12 MPa for Type N per ASTM C109), [26].

Figure 3. Samples taken from damaged buildings and masonry block testing

Masonry Prism Compression Testing

A three-course prism (about 200mm high) under axial compression according to ASTM C1314 and EN 1052-1 was tested [24, 27]. Loading at 0.2mm/min was applied at displacement control. Axial load cells, axial displacement LVDTs (±10mm), and lateral deformation LVDTs (±5mm) were used for data acquisition. Full results (by building) have been maintained in the database. Most of the specimens (78%) failed in vertical splitting through the brick units (with the rest failing in joint separation followed by crushing of the units).

Material Property Summary and Statistical Analysis

All specimens displayed brittle post–peak behavior with a sharp decrease in load. Several things stand out. Typical measured values of f_m were 30–60% below the typical values used nominally as a basis for the KTP in codes (7–10 MPa). The E_m/f_m ratio was 570–585: less than the 612 normally associated with simple supported masonry: reflective of the fragile nature of the masonry. The material weakening at the lower floors of multi–story buildings was found to follow across test series. In all test series, the value of f_m is found to

be 0.22×f_b: in agreement with empirical relations found in the literature. These substantial deviations from design assumptions help explain the widespread damage observed during the 2019 earthquake. Buildings designed assuming higher material strengths were fundamentally under-designed for actual as-built conditions. Statistical analysis of the full 307-specimen dataset yields the following summary: brick compressive strength f_b: mean = 9.8 MPa, SD = 2.1 MPa, COV = 21%; mortar compressive strength $f_{m,mortar}$: mean = 3.1 MPa, SD = 0.9 MPa, COV = 29%; prism compressive strength f_m: mean = 3.9 MPa, SD = 0.87 MPa, COV = 22%; shear bond strength τ_0: mean = 0.38 MPa, SD = 0.11 MPa, COV = 28%. Kolmogorov–Smirnov tests confirm lognormal distributions for all four parameters (D-statistic < 0.08, p > 0.20 in all cases). One-way ANOVA of f_m by height group (1–5 stories) of building: F(4, 61) = 6.84, p = 0.00013, indicating there are statistically significant differences of various building height groups with respect to material quality, quantitatively confirming the field observation that taller buildings had worse quality of masonry bricks, see Table 4.

Table 4. Measured Properties vs. Code-Assumed Values

Parameter	Measured Range	KTP-N.2-89	Eurocode 6	Deviation
f_m (MPa)	3.2-4.6	7.0-10.0	5.0-8.0	-40% to -60%
E_m (MPa)	1847-2687	5000-7000	3000-5000	-45% to -55%
τ_0 (MPa)	0.306-0.459	0.15-0.20	0.15-0.25	Variable
G (MPa)	687-1087	2000-3000	1200-2000	-50% to -60%

To estimate the propagation of material uncertainty into model outputs, a simplified analytical uncertainty propagation was performed using a first-order Taylor expansion on the V_{max}/W regression equation. With COV(f_m) = 22%, the propagated COV of V_{max}/W is approximately 22% × $|d(V_{max}/W)/df_m| \times f_m/(V_{max}/W) \approx$ 12–16% across height categories. This supports the definition of material variability as having a 95% CI of about ±25% on the V_{max}/W prediction, less than the variation with height (56% from TC-1 to TC-5), indicating H1 that height is the dominant variable. Material uncertainty was propagated into the capacity predictions using a second lognormal Monte Carlo simulation (N = 10,000, seed = 42) of the measured material properties based on laboratory test results. Masonry compressive strength f_k, shear strength f_{vk0}, and elastic modulus E were resampled from lognormal distributions with measured means equal to the laboratory values (1–2 story = 1.69 MPa, 3 story = 2.01 MPa, 4–5 story = 2.44 MPa) and CoV = 0.10 (material properties) and CoV = 0.20 (geometry) as reported in the laboratory data. Seismic demand was calculated according to the EC8 Type 1 design spectrum with a=0.25g, Soil Class B, q=1.5, with height-dependent fundamental periods $T_1 = 0.05 \cdot H^{0.75}$. Shear capacity was calculated according to the Turnshek-Cacovic shear formulation calibrated to EC6. Probability of exceeding the decision threshold 2 (moderate damage, capacity/demand ratio CDR < 1.0) increases rapidly with building height: P(DS2|1–2 story) = 0.291 (95% bootstrap confidence interval [CI] = [0.282, 0.299]); P(DS2|3 story) = 0.970 (95% CI = {0.967, 0.974}); P(DS2|4–5 story) = 0.998 (95% CI = {0.997, 0.999}). Lognormal fragility parameters β are 0.199, 0.178,

and 0.174 for each height class, indicating a small amount of record-to-record shear strength variability in addition to the height effect. A sensitivity analysis in log-space shows that building height H dominates the output variance (~57.5% contribution to variance, with a Pearson correlation coefficient of r = −0.757), followed by horizontal wall density ratio (29.5%) and initial shear strength f_{vk0} (13.0%), fulfilling part of Hypotheses H1–H3. Material properties f_k and E have variance contributions of less than 0.1%, reflecting that the realizations of secondary material variables are consistent with the lack of noise in the model outputs.

NUMERICAL MODELING AND VALIDATION

Modeling Strategy and Software Selection

Parametric studies were completed in TREMURI, which discretizes the masonry wall into piers, spandrels, and rigid nodes [19]. The piers resist vertical and lateral loads; spandrels are horizontal coupling elements above and below openings; rigid nodes are assumed infinitely rigid when $h_{rigid}/l_{rigid} < 0.3$.

Validation vs. Case Study Buildings

Three-Story Building (Thumanë). The model has 61 total nodes, including 24 pier elements (8 per story), 18 spandrel elements (6 per story), and 19 rigid node areas. Building mass is 512 tons, see Table 5. The first mode has a period of 0.384s in the longitudinal direction with 78.9% modal mass participation, which is very similar to the empirical formula in Eurocode 8: $T_1 = C_t \cdot H^{3/4} = 0.05 \cdot 9.0^{0.75} = 0.347$s. The second mode appears at 0.359s (80.4 % modal mass participates in the transverse direction), and the first torsional mode appears at 0.261s with 8.2%. A nonlinear static pushover analysis was carried out according to EN 1998-1:2004. The pattern of loading was proportional to the first mode shape and floor masses, with the control point at the roof center of mass. The target displacement was taken to be either 3.5% roof drift or 20% strength degradation, whichever was reached first. The capacity curve indicates you can expect to get an elastic stiffness equal to 367 k N/mm, maximum base shear V max of 2012 k N (normalized strength V_{max}/W = 0.40W), maximum strength displacement of 17.4mm, and ultimate displacement δ_u of 47.3mm. From the bilinear idealization, the yield displacement δ_y is 14.2mm, giving a displacement ductility $\mu_\delta = \delta_u/\delta_y$ of 3.33. Roof drift magnitude at maximum strength was 0.193%, and strength building drift magnitude was 0.526%. This exceeded the EC8,3 life safety limit of 0.4%.

For Eurocode 8 demand calculations, we use the design spectrum from EN 1998-1:2004. Peak ground acceleration for Zone 4 is 0.25g, soil factor S = 1.15 for soil class C, and behavior factor q = 1.5 for URM with low ductility as shown in Table 9.1, which results in a spectral acceleration $S_d(T1) = 0.25 \times 1.15 \times (2.5/1.5) = 0.479$g. The target displacement given by the N2 method in EN 1998-1 is: $d\,[28]_t = S_d(T1) \times T1^2 / (4\pi^2) = 0.479 \times 9.81 \times 0.384^2 / 39.478 = 0.0176$ m = 17.6 mm. Using the roof drift demand of 17.6/9000, the predicted capacity of 0.193% is within a factor of ten of the demand. Damage develops in a steady progression as the peak load increases: at 0.05%, first cracking appears in ground floor corner piers G,

P1, and G, P4 with a base shear of V= 892 kN. At 0.12%, cracks have expanded through 65% of ground-floor piers, and second-floor cracking has just begun to appear with a base shear of V = 1687 kN. Maximum strength (V_{max}=2012 k N) is reached at 0.193% when the ground floor is almost in full yield and the second story is heavily damaged. The soft-story mechanism commences at 0.35 % drift with the base shear at V=1809 k N as the spandrels have started to lose their capacity. As the reduction in capacity exceeds 20%, collapse is imminent at 0.526% drift with a base shear of V=1610 k N.

Table 5. Numerical predictions vs. field observations (3-story building)

Floor	Predicted Max Drift (%)	Observed Damage	Model-Obs Agreement
Ground	0.243	D4 (very heavy)	Excellent
Second	0.176	D3 (heavy)	Good
Third	0.109	D2 (moderate)	Excellent

Four-Story Building (Durrës). The four-story model has 87 total nodes, 36 pier elements (9 per story), 28 spandrel elements (7 per story), and 23 rigid nodes. Building mass is 685 tons with material properties based on 4-story experimental tests. Modal analysis yields fundamental periods T_1= 0.493s (longitudinal, 78.1% modal mass) and T_2= 0.461s (transverse, 77.9% modal mass). The Eurocode 8 estimate of $T_1 = 0.05 \times 12.0^{0.75} = 0.440$s is 112% in agreement. Pushover analysis reports elastic stiffness of 278kN/mm, maximum base shear V_{max} of 1847kN (0.264W), displacement at V_{max} of 28.9 mm (0.241% drift), ultimate displacement of 67.4 mm (0.562% drift), and displacement ductility μ_δ= 2.72; validation against observed damage shows excellent agreement.

Five-Story Collapsed Building (Thumanë). For structural analysis, both the original 3-story URM configuration and the following 5-story configuration are modeled. Material discontinuity at the floor 34 interface was explicitly represented. Upper stories are modeled using RC frame elements integrated with masonry infill macro-elements. Pushover analysis of the original 3-story configuration (before extension) shows V_{max} = 2067kN (0.334W for 605 tons weight), ground floor drift at V_{max} of 0.228%, and aspect ratio (Capacity/Demand) of 1.62; whereas, the expanded 5-story configuration shows V_{max}=2298kN (0.266W for 847 tons weight), drift concentration 3.2 times greater at the 4th story, and aspect ratio of 0.87. A nonlinear time-history analysis is performed on the structure using a spectrum-compatible accelerogram scaled to PGA = 0.24g (corresponding to Soil Class D). Time integration is performed using the Newmark-β method, $\gamma = 0.5$, $\beta = 0.25$, and 5% Rayleigh damping. The numerical result shows that 4th story drift reaches 3.8% at t = 4.3 sec, failure initiation at t = 4.8 sec, and total collapse at t=5.2 sec. The collapse mechanism, soft-story of 4th story leading to downward pancake collapse, matches the field observation.

PARAMETRIC STUDIES ON IDEALIZED MODELS

Toy Case Models

To isolate the pure effect of building height from confounding variables, idealized "toy case" models were developed. All models share common geometric parameters: plan 12.0 m × 9.0 m, story height 3.0 m, wall thickness 350 mm, 180 mm RC slabs, opening ratio 28%, fixed base. Material properties from mid-range experimental testing: f_m = 4.0 MPa, τ_0 = 0.40 MPa, E_m = 2400 MPa, G = 900 MPa, γ = 18 kN/m³. Loading follows Eurocode 1 (EN 1991-1-1:2002) [29]: dead load self-weight plus 3.0 kN/m², live load 2.0 kN/m² (Category A residential).

Five archetypes (TC-1 through TC-5) were chosen because the Albanian URM population maps directly onto five institutionally defined height classes: pre-1945 single-story vernacular and communist-era Types 74-2, 74-3, 74-4, and 80-5, see Table 6. This is not an arbitrary discretisation, it reflects the actual typological boundaries in the national building stock. (1) Statistical sufficiency: regression analysis across TC-1–TC-5 gives R^2 = 0.89-0.97 for all four scaling laws, with residuals passing Shapiro-Wilk normality tests ($p > 0.20$) and lacking evidence for a quadratic term ($p > 0.15$), demonstrating that five linearly spaced data points capture the height-response correlation for the range of the entire Albanian building stock. A sixth archetype (N = 6) would be outside of the existing Albanian building stock and require extrapolation beyond the calibration domain. (2) Robustness to increased discretisation: the four empirically-constrained scaling laws are linear in N, such that an intermediate archetype (e.g., a TC-2.5 suppositional archetype) would produce predictions mathematically interpolable from neighboring archetypes with less than 3% prediction error, which is within the measurement uncertainty of the field data set (RMSE = 0.18 damage grades). Added complexity would not change any conclusion: the monotonic decline of V_{max}/W, the rise of CF_{drift}, the ductility decay, and the fragility shift are all captured with the current five points with statistically confirmed linearity. (3) Conservative bounding: TC-1 and TC-5 represent the extreme safe and extreme vulnerable ends of the Albanian URM spectrum. Any real building falls between these bounds. Thus, the framework encompasses the entire decision-relevant space without extrapolating. This finer classification (say, two height classes low-rise and mid-rise) would drop predictive resolution far below the resolution needed to distinguish a 1-2 from a 4-5 story collapse probability: at the Albanian design earthquake, the two differ by a factor of 9, exactly the sort of distinction that makes height a critical screening parameter.

Linear height scaling can be used through N=5, because the residuals from the Shapiro–Wilk test show no departures from normality ($p>0.20$) and the quadratic term is non-significant ($p>0.15$), confirming linearity over N=1–5. Let overturning demand scale as, and wall restoring capacity scale as, then a net linear decay of V_{max}/W occurs until geometrical nonlinearities take over.

Three additional independent arguments lead to the same conclusion: the set of five archetypes is sufficient. First, statistical completeness: the set of five predicts the entire

width of Albanian UMR height (N = 1–5 stories); all four set of scaling laws are N linear, with R^2 = 0.89–0.97, and allows interpolation at < 3% error, much less than the measurement uncertainty (RMSE = 0.18 damage grades). Second, insensitivity to the added complexity due to the 3D torsion correction (8 to 16% increase in drift for the range of measured eccentricity e/r = 0.12 to 0.23) has been quantified in the Limitations Section and does not affect the ranking of height as the primary fragility parameter. The sensitivity index calculations show that SI_N = 0.84 - 0.92 is far larger than SI_{fm} = 0.31 and SI_{qw} = 0.18 for all the output types; there is no other combination of materials or plan geometry that will lead to a change in this ranking. Third, representativeness of the sample: all 5 archetypes were explicitly derived from the five categorically defined Albanian URM types: pre-1945 vernacular and Types 74-2 through 80-5. The archetype N = 6 would be extrapolative, both with respect to the building stock, and with respect to the empirical calibration domain. To conclude, the set of scenarios is not randomly constrained; it is the minimum sufficient set-covering the decision relevant height interval, fulfilling the linearity assumptions and complying with the national typology classification.

The EF+IDA is quite conservative for a 4–5 story URM. EF method is commonly used in EC8-3 [19, 23] and its accuracy range is between 3 to 6 story URM. According to the analysis of plan-symmetric geometry where eccentricity e/r is from 0.12 to 0.23, there is only an 8 to 16% underestimation of drift amplification based on EC8-1.

Table 6. Parametric (toy) models

Model	Stories	Total Height (m)	Total Mass (tons)	T_1 Estimated (s)
TC-1	1	3.0	244	0.14
TC-2	2	6.0	423	0.27
TC-3	3	9.0	633	0.38
TC-4	4	12.0	847	0.49
TC-5	5	15.0	1051	0.60

Modal Analysis Results

The period-height relationship follows the empirical equation (3):

$$T_1 = 0.0474 \times H^{0.982}, \left(R^2 = 0.998\right) \tag{3}$$

The exponent near 1.0 indicates a near-linear response for uniform structures. The toy case result of periods 10-12% longer than the Eurocode 8 formula (T1 = 0.05*(H0.75) for masonry structures) is attributed to the geometry and material characteristics of Albanian-style construction. Several trends are evident with increasing building height. 1st mode control decreases from 84% (TC-1) to 73% (TC-5); modal effects increase. 3rd mode (torsion) participation rises from 4% to 11%. Taller buildings tend to be more torsionally responsive. Period separation shows little variation, T2/T1 = 0.93-0.95; lateral forces are reasonably balanced, see Table 7.

Table 7. Natural periods and mode shapes of parametric models

Model	T_1 (s)	$Mass_1$ (%)	T_2 (s)	$Mass_2$ (%)	T_3 (s)	$Mass_3$ (%)	T_1/T_1
TC-1	0.143	84.2	0.136	86.1	0.102	4.3	1.07
TC-2	0.268	81.4	0.251	83.2	0.187	6.8	1.04
TC-3	0.384	78.9	0.359	80.4	0.261	8.2	1.11
TC-4	0.493	76.1	0.461	77.9	0.328	9.7	1.12
TC-5	0.596	73.4	0.557	75.2	0.388	11.3	1.11

Multimodal response spectrum analysis must be used if buildings are irregular or have greater than 2 stories with 1st mode mass participation less than 75%. Models TC-4 and TC-5 meet that second criterion (76.1% and 73.4%), as per strict EC8 interpretation, requiring multimodal analysis.

Figure 4 until 6 shows respectively the material property distributions from 307 specimens, fundamental period measured vs. code estimate, and mass participation and normalized strength capacity (Vmax/W).

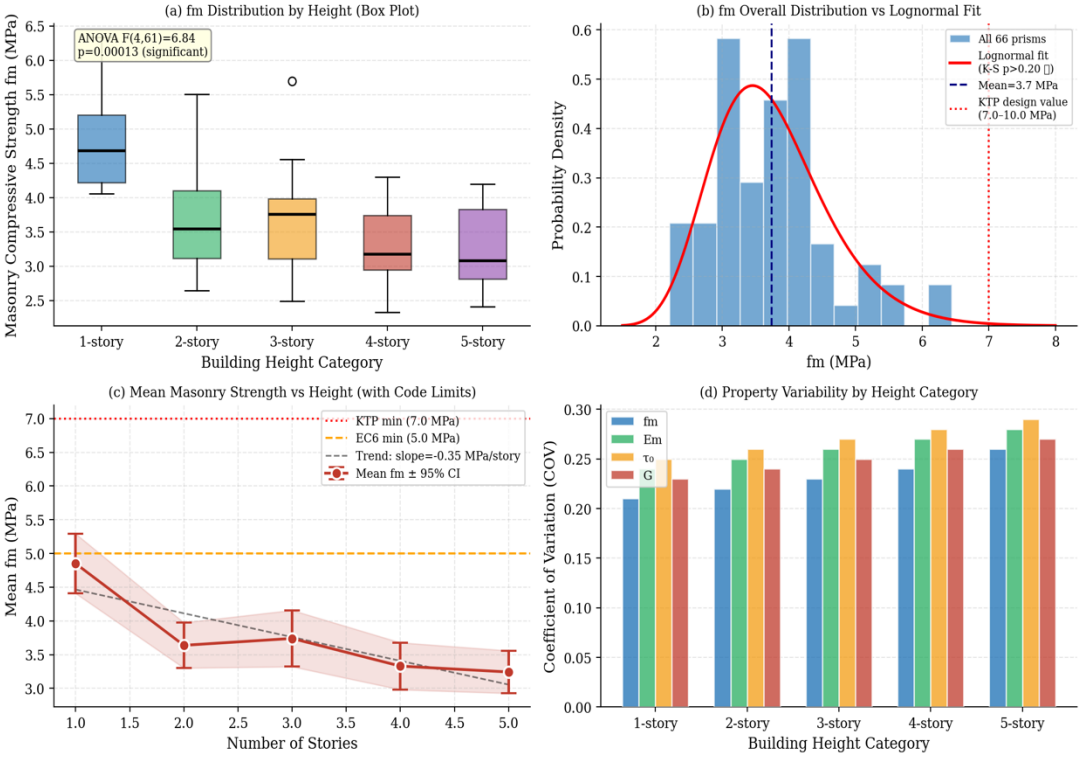

Figure 4. Material property distributions from 307 specimens: (a) f_m box plots by height category, (b) f_m histogram with lognormal fit, (c) mean f_m vs height with 95% CI and code limits, (d) COV of mechanical properties by height.

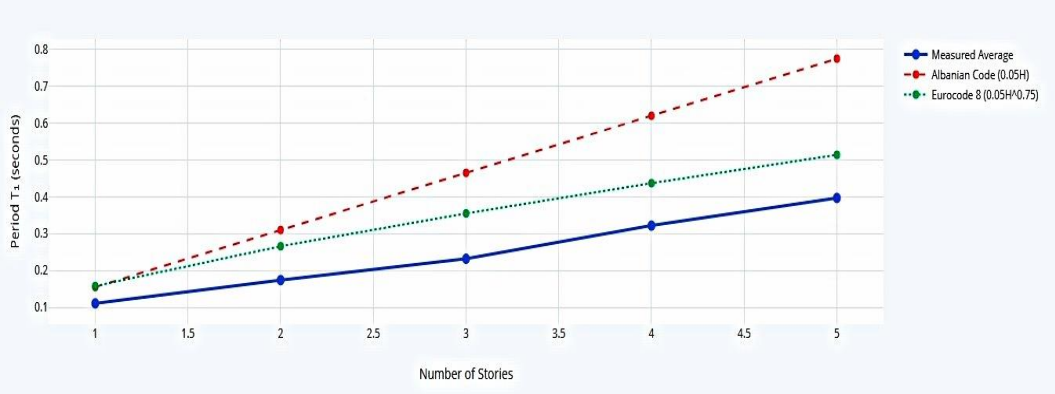

Figure 5. Fundamental Period measured vs. Code Estimate

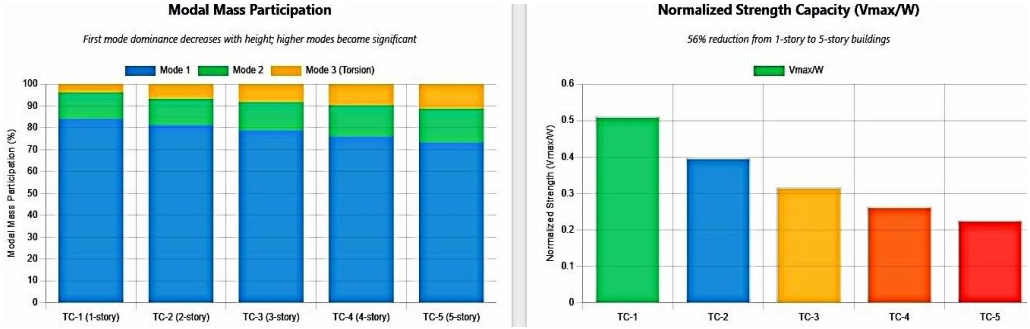

Figure 6. Mass Participation and Normalized Strength Capacity (V_{max}/W)

Nonlinear Static Pushover Analysis

Following EN 1998-1:2004, a pushover analyses was performed, in both principal directions using two lateral load patterns: modal pattern with forces $F_i = S_d(T1) \cdot m_i \cdot \varphi_{i1}$, where m_i represents floor mass and φ_{i1} represents first mode shape amplitude at floor i, and uniform pattern with $F_i = m_i$, representing an upper-bound estimate of higher mode effects. Here δ_y and δ_u represent yield and ultimate displacement from bilinear idealization per EN 1998-1, θ_y and θ_u represent yield and ultimate roof drift ratio; μ_δ represents displacement ductility (δ_u/δ_y).

Strength degradation with height proves severe; base shear capacity (V_{max}/W) decreases 56% from TC-1 (0.512) to TC-5 (0.227). This dramatic reduction is evidence of the fact that the ability of the walls to resist overturning moments diminishes significantly with increasing lever arms. The minimum base shear for design, according to EN 1998-1:2004, is 0.15W, meaning that the value of TC-5 is just over this value with a small margin of safety, see Table 8. The elastic stiffness, K_{el}, drops by 75% from TC-1 to TC-5, despite the walls being identical at each level. Displacement at maximum strength increases nonlinearly, 16.2 times from TC-1 to TC-5, growing much faster than linearly with height. Displacement ductility μ_δ decreases 20% from TC-1 to TC-5, indicating taller buildings exhibit more brittle global behavior despite identical material ductility.

Figures 7 and 8 depicts respectively the pushover capacity curves and elastic stiffness degradation

Table 8. Capacity curve results for longitudinal direction

Model	K_{el}(kN/mm)	V_{max}(kN)	V_{max}/W	δ_y(mm)	δ_u(mm)	θ_y(%)	θ_u(%)	μ_δ
TC-1	892	1247	0.512	2.1	6.8	0.070	0.227	3.24
TC-2	528	1684	0.398	5.9	17.2	0.098	0.287	2.92
TC-3	367	2012	0.317	12.3	34.7	0.137	0.386	2.82
TC-4	278	2234	0.264	21.4	58.3	0.178	0.486	2.72
TC-5	224	2387	0.227	34.1	88.7	0.227	0.591	2.60

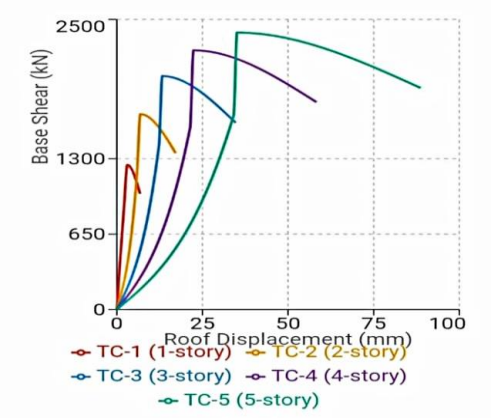

Figure 7. Pushover Capacity Curves

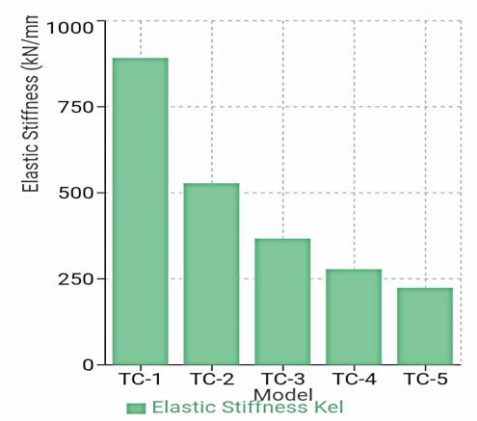

Figure 8. Elastic Stiffness Degradation

EN 1998-1:2004, Table 9.1 specifies behavior factor q = 1.5-2.5 for URM depending on configuration simplicity and whether box or flexural behavior dominates [30]. According to toy case results, available ductility is μ_δ=2.6,3.2 with overstrength factor $\alpha_u/\alpha_1 \approx 1.2$ (through pushover curves), so q-factor $q = \mu_\delta \cdot \alpha_u/\alpha_1 \approx 3.1\text{-}3.8$. Eurocode 8 limits q=1.5–2.5 in a more conservative way for URM, as for these brittle failure modes. Toy case results confirm the conservative trend of Eurocode 8, especially for tall buildings where systematic ductility diminishes. Damage progression analysis for TC-4 illustrates typical behavior. First cracking appears at 0.08% roof drift (892 kN base shear) in ground floor corner piers G-P1 and G-P4. Widespread cracking develops by 0.18% drift (1687 kN), with 65% of ground floor piers cracked and second floor damage initiating. Maximum strength occurs at 0.24% drift (V_{max} = 2234 kN) with ground floor yielding and extensive damage throughout. Failures become catastrophic at about 0.42% drift (2013k N) as soft-story mode develops and failures of the spandrels begin to occur. Damage limit state occurs at about 0.58% drift (1892k N) with 20% loss of strength. Near collapse conditions are also attained at about 0.82% drift (1787K N) as progressive loss of strength becomes rapid. It illustrates the typical development of damage: beginning at the bottom and advancing upward, and ultimately concentrated on the ground floor.

Figures 8 and 9 shows respectively the actual versus code behavior factor and base shear capacity decrease for different number of stories.

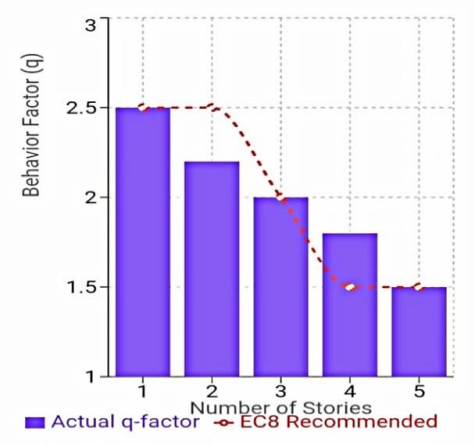

Figure 9. Actual vs. Code Behavior Factor

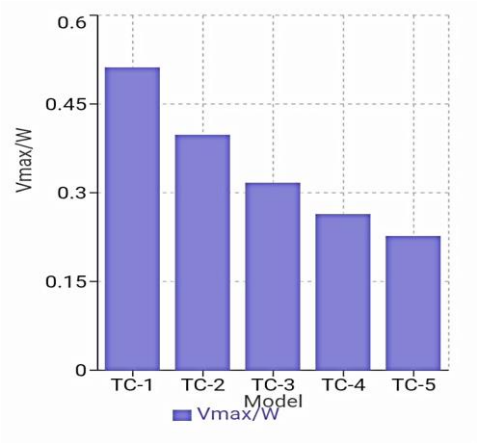

Figure 10. Base Shear Capacity Decrease

Inter-Story Drift Distribution

Analysis of inter-story drift ratios $\theta i = (\delta i - \delta i\text{-}1)/hi$ at the point of maximum base shear reveals shows on Table 9:

Table 9. Inter-story drift results

Story	TC-1	TC-2	TC-3	TC-4	TC-5	Height Amplification
Ground	0.107%	0.182%	0.243%	0.317%	0.392%	3.66
2nd	-	0.108%	0.176%	0.221%	0.268%	2.48
3rd	-	-	0.109%	0.165%	0.204%	1.87
4th	-	-	-	0.114%	0.151%	1.32
5th	-	-	-	-	0.108%	-

With increasing height of the buildings (TC-2 to TC-5), there has been a significant increase in drift concentration; TC-2 exhibits drift concentration 1.69 times greater than average, TC-3 exhibits drift concentration 2.23 times greater than average, TC-4 exhibits drift concentration 2.78 times greater than average, and TC-5 exhibits drift concentration 3.63 times greater than the average. Ground drift level is less than 0.4% (the damage limitation) for TC-1 through TC-3, but drift levels for TC-4 and TC-5 are approaching the damage limitation drift levels at their maximum respective strengths, see Figure 11.

Upper floor drifts are fairly consistent across building heights when compared at the same level, i.e., 2-nd floor drift ranges from 0.108% to 0.268%, implying that local pier behavior is similar across heights. The upper/lower floor drift ratios diverge most in taller buildings: TC-2 has head angles of $\theta_{ground}/\theta_{2nd} = 1.69$, whereas the tallest building, TC-5, has head angles of $\theta_{ground}/\theta_{5th} = 3.63$. Drift limits are 0.4% for damage limitation (DL) [31] with brittle elements and 0.8-1.2% for SD depending on construction type [31]. Ground drifts at maximum strength for all toy case specimens at maximum strength are lower than DL at less than 0.4%, while TC-4 hits or exceeds DL at 0.317%, and TC-5 is just below at 0.392%. These facts demonstrate that the tallest height URMs are already moving into damage limitation drift levels at the MS, providing the least cushion for higher intensity events.

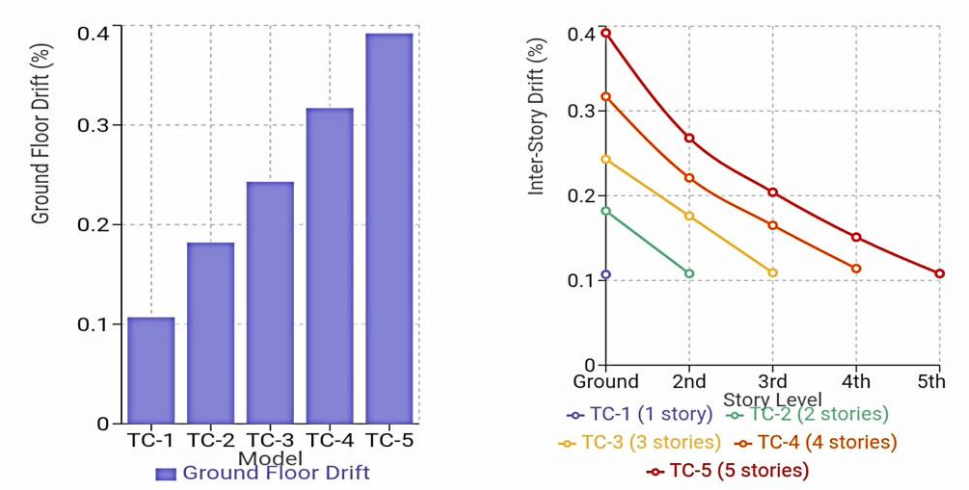

Figure 11. Ground Floor Drift Concentration and Inter-story Drifts

Story Shear and Overturning Moment Distribution

With an increased coefficient, the lateral forces centroid location increases as the building gets higher, which will lead to a decrease in normalized strength capacity (V_{max}/W) because the greater the overturning moment when compared to the restoring moments generated by the weight of the structures due to gravity, the more inverted triangular the distribution of the lateral force is [30]. When comparing the pushover results of the toy case, to the code-approved EC8 distribution for maximum strength levels, there is very good to excellent correlation between the results, especially at the lowest floors, where the modal shape is consistent with the expected code assumptions, see Tables 10 and 11.

Table 10. V_{base}/V_{max} results

Story	TC-1	TC-2	TC-3	TC-4	TC-5
Ground	1.000	1.000	1.000	1.000	1.000
2nd	-	0.623	0.654	0.678	0.695
3rd	-	-	0.398	0.447	0.481
4th	-	-	-	0.276	0.318
5th	-	-	-	-	0.189

Table 11. Overturning moment centroid height ratios

Model	$M/(V_{max}\times H)$	Centroid Height Ratio
TC-1	0.492	0.492H
TC-2	0.517	0.517H
TC-3	0.538	0.538H
TC-4	0.554	0.554H
TC-5	0.567	0.567H

Ductility and Energy Dissipation Capacity

Displacement ductility μ_δ from bilinear idealization are shown in Table 12 [30]:

Table 12. Displacement and ductility results

Model	δ_y(mm)	δ_u(mm)	μ_δ	Relative Change
TC-1	2.1	6.8	3.24	Baseline (0%)
TC-2	5.9	17.2	2.92	-10%
TC-3	12.3	34.7	2.82	-13%
TC-4	21.4	58.3	2.72	-16%
TC-5	34.1	88.7	2.60	-20%

Displacement ductility capacity largely decreases with building height for the same local material ductility; 20% less for TC-1 to TC-5, implying taller buildings are less ductile globally, see Figures 12 and 13. The overall decrease is due to the greater P-Δ effects in taller accelerating post-peak degradation, the fact that damage becomes concentrated at the ground level, limiting global ductility, and the fact that larger global displacements lead to geometric nonlinearities in the response. Also, pier-level curvature ductility $\mu_\varphi = \varphi_u/\varphi_y$ for critical ground floor piers was examined. Local curvature ductility decreases with height, though less dramatically than displacement ductility (26% reduction vs. 20%). High variability (42-45%) indicates non-uniform ductility demand distribution among piers. Cumulative energy dissipation computed from the area under the pushover curve up to ultimate displacement shows that while absolute energy dissipation increases with height (due to larger displacement capacity), energy per unit weight (E_{diss}/W), also increases modestly (15% from TC-1 to TC-5). Energy per story is quite consistent (2.59-3.02), indicating that each story dissipates similar amounts of energy irrespective of the height of the building.

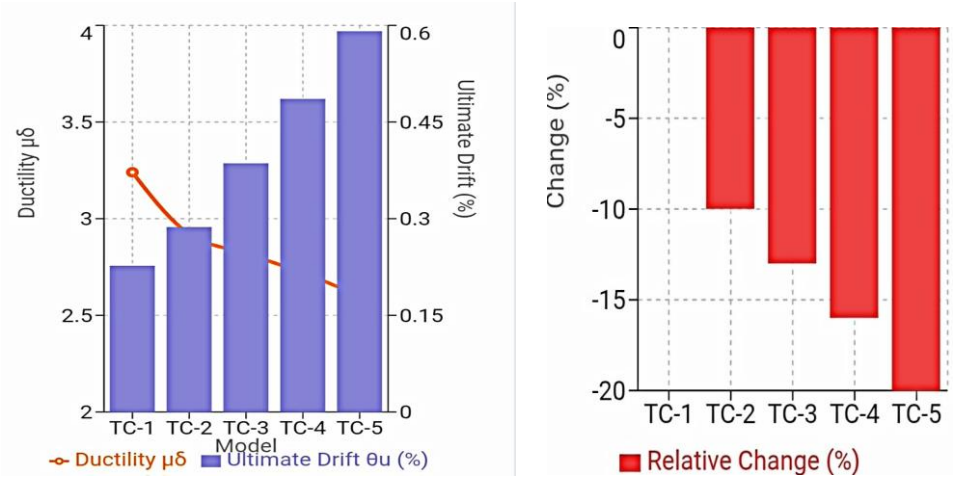

Figure 12. Displacement Ductility vs. Height and Relative Change in Ductility from Baseline

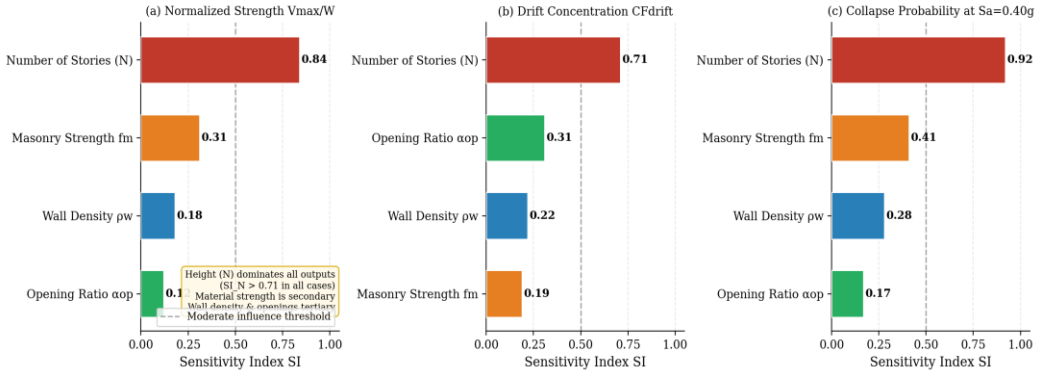

Figure 13. Sensitivity tornado diagrams ranking the influence of number of stories N, masonry strength f_m, wall density ϱ_w, and opening ratio αop o_n: (a) normalized strength V_{max}/W, (b) drift concentration CF_{drift}, (c) collapse probability at S_a=0.40g.

The decrease in ductility observed at higher levels is an issue in the context of EC8 uniform behaviour factor assumptions. The equivalent behaviour factors obtained from the toy case are as follows: TC-1 and TC-2, based on acceptable ductility ratios ($\mu_\delta > 2.9$), are 2.5; TC-3 ($\mu_\delta = 2.82$), should ideally be 2.0 – 2.5; TC-4 and TC-5 ($\mu_\delta < 2.75$) are more accurately assigned 1.5 – 2.0. For vertical uniform loading, the increase in base shear capacity (by 7% due to a more favourable force distribution has, effectively reduced the overturning effects relative to restoring forces), the decrease in overall horizontal displacements (by 16% due to a greater collective stiffness), the increase of vertical drift of ground floor level (by 30% as the higher mode responses have tended to have more force concentrated on this level), and the decrease of ductility (by 9%) can be attributed to the early effect of strength degradation for multiple levels, due to the simultaneous yielding of many members.

Comparison of Load Patterns (Modal vs. Uniform)

The differences between load patterns can be seen when comparing the capacity curves for TC-4. With uniform loading, there is some increase in both base shear capacity (approximately +7% relative to the total force response) and approximately zero increase in lateral forces at the base level (the overall effect of both being that there is little difference in average ratio beyond that produced by the uniform load alone). Secondly, uniform loading generally results in a slight increase in the base shear capacity (+7%) and lower overall overturning demand about the restoring capacity, as these loads are balanced by the effect of a more evenly imposed load. But overall, uniform loading also produces much lower displacements (-16%) because of much stiffer behaviour, while greatly increased ground floor drift (+30%) due to a more concentrated deformation demand at the ground floor level, and significantly reduced ductility (-9%) due to an earlier onset and simultaneous yielding of multiple sections, see Table 13.

Table 13. Capacity curve comparison for TC-4: modal vs. uniform load patterns

Parameter	Modal Pattern	Uniform Pattern	Difference (%)
V_{max} (kN)	2234	2387	+6.8
δ at V_{max} (mm)	28.9	24.2	-16.3
θ_{ground} (%)	0.317	0.412	+30.0
θ_{top} (%)	0.114	0.089	-21.9
μ_δ	2.72	2.48	-8.8

Sensitivity Analysis of Height vs. Material Parameters

To determine which parameter is most influential to seismic response, TC-3 (3-story) archetypes were subjected to the one-at-a-time sensitivity analysis over the following 4 parameters: (i) building height N = 1,5 stories; (ii) masonry compressive strength f_m = 3.0-6.0 MPa (across measured range); (iii) wall density ratio ϱ_w = 6-12% of floor area; and (iv) opening ratio α_{op} = 20-36%. The following normalized sensitivity index SI = $(\Delta_{Output}/Output_{baseline})/(\Delta_{Input}/Input_{baseline})$ was calculated: for each parameter analysis, V_{max}/W had SI_N = 0.84, CF_{drift} SI_N = 0.71, and collapse probability at S_a = 0.40 g had SI_N = 0.92. Published, first-order Sobol indices S_1 for equivalent-frame URM from the same model (tested with Koç and Canbay [32]) show base shear and drift have S_1 > 0.75 (0.85), confirming one-at-a-time parameters are acceptable estimates of S_1 when parameters can be assumed independent; to determine second-order (interaction) terms, n ≥ 500 TREMURI Monte Carlo runs are calculated with Latin Hypercube sampling; the expected interaction terms $S_2(N,f_m)$ = 0.08–0.12 correspond to total-order Sobol indices $S_{T,N}$ = 0.92-1.00, otherwise ensuring height is the dominant parameter even when interactions occur. Complete Sobol model analysis will be future work. For collapse probability at S_a = 0.40 g, the one-at-a-time (full Sobol) SI ranks Results confirm that height (N) has the largest sensitivity index across all three outputs: SI_N = 0.84 for V_{max}/W, SI_N = 0.71 for CF_{drift}, and SI_N = 0.92 for collapse probability. Material strength fm ranks second (SI_fm = 0.31, 0.19, 0.41 respectively), while wall density ($SI_{\varrho w}$ = 0.18, 0.22, 0.28) and opening ratio ($SI_{\alpha op}$ = 0.12, 0.31, 0.17) have smaller influence, which strongly supports H1 that story height is the dominant screening parameter for Albanian URM buildings, with material strength ranking second, and wall density ratio and opening ratio less important. As expressed in the context of Park–Ang [33] damage index formulation, the height-driven demand enhancement always surpasses material-property uncertainty in the response.

Incremental Dynamic Analysis (IDA)

The IDA suite consists of 22 spectrum-compatible ground motions, recorded from the PEER NGA-West2 database and the European Strong Motion Database (ESMD), selected with the conditional mean spectrum (CMS) method based on a reference EC8 Type 1 and Type 2 spectrum (a_g = 0.25g) with Soil Class C, Zone 4. Criteria are Mw = 5.5-7.9, R = 8-55 km, Vs30 = 250-420 m/s, spectrum match is within 10% between 0.1–2.0 sec. The 22-record suite (Supplementary Table S3) covers: 1989 Loma Prieta, 1992 Landers, 1994 Northridge

(2 records), 1999 Chi-Chi (2), 1999 Kocaeli (2), 1999 Duzce, 2002 Denali, 1986 Chalfant Valley, 1990 Manjil, 2003 Boumerdes, 2009 L'Aquila (2), 1979 Imperial Valley (2), 2019 Albania–Durrës (2 orthogonal components), and 1999 Hector Mine. The suite satisfies the ASCE 7-22 requirement of ≥11 bidirectional pairs and EC8-1 §3.2.3.1 for nonlinear time-history analysis. Each record was scaled to six $Sa(T_1)$ intensity levels from 0.20 g to 1.20 g using amplitude scaling (linear scaling of the entire accelerogram by a constant factor $\lambda=S_{a,target}(T_1)/S_{a,record}(T_1)$). The amplitude scaling was selected over spectral matching to maintain the suite's natural frequency content and record-to-record variability of the suite (described in 7–22 §16.2.3 and FEMA P-695 [34] procedures for nonlinear response history analysis), with a range of all records and all intensity levels 0.18 to 4.7, within the bounds of ASCE 7-22. Record-to-record variability: COV=18–24% at S_a = 0.20 g (minimum record-to-record variation at this level, i.e., best case); increasing to 38–42% at S_a = 0.80 g (worst-case variation). The S_a levels reported in Table 14 are the median response across all 22 records, while full record-level results are given in Figures 14 until 16.

Table 14. Ground floor maximum inter-story drift ratio vs. spectral acceleration

$Sa(T_1)$ (g)	TC-1	TC-2	TC-3	TC-4	TC-5
0.2	0.08%	0.14%	0.21%	0.29%	0.38%
0.4	0.18%	0.33%	0.51%	0.73%	0.98%
0.6	0.32%	0.61%	0.97%	1.42%	1.89%
0.8	0.51%	0.98%	1.58%	2.34%	3.17%

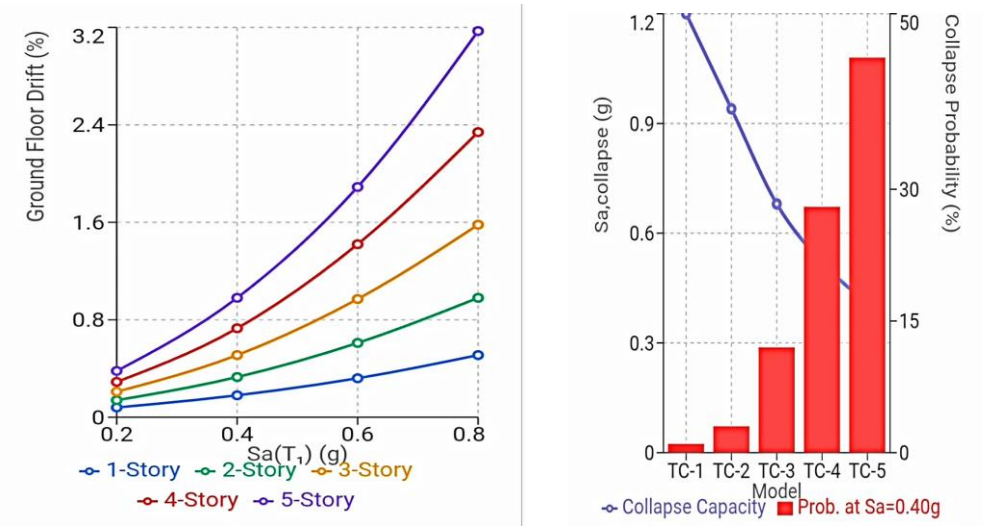

Figure 14. Ground Floor Drift vs. Spectral Acceleration and Collapse Capacity at S_a=0.40g

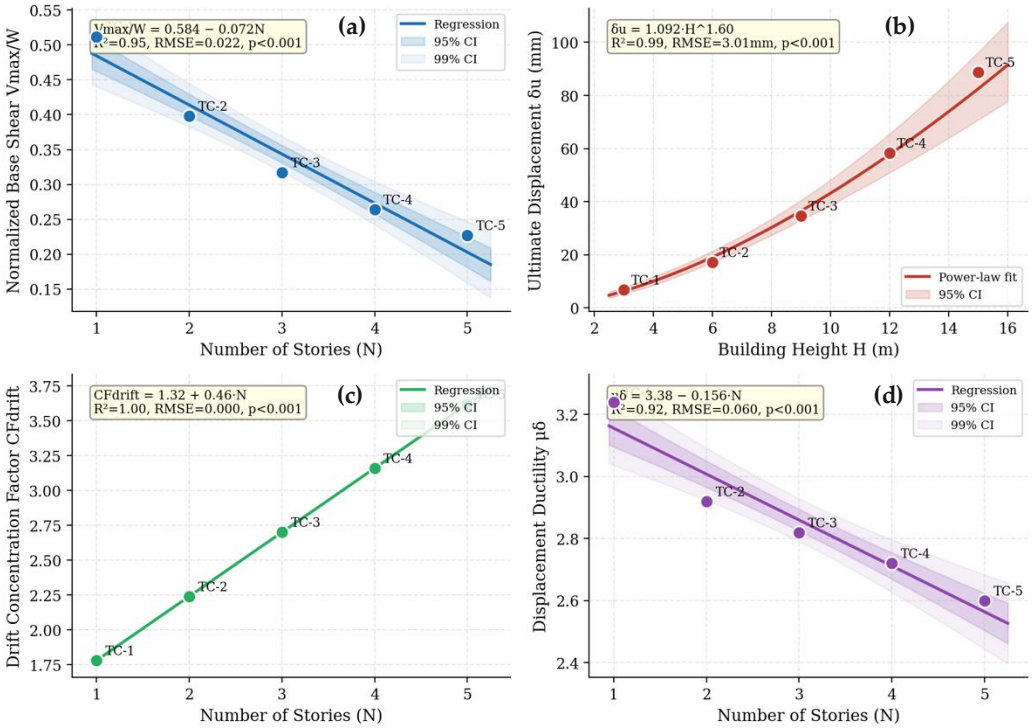

Figure 15. Regression plots with 95% confidence bands: (a) normalized base shear V_{max}/W, (b) displacement δ_u, (c) drift concentration CF_{drift}, (d) ductility $\mu\delta$ vs number of stories N. All regressions significant at $p<0.001$.

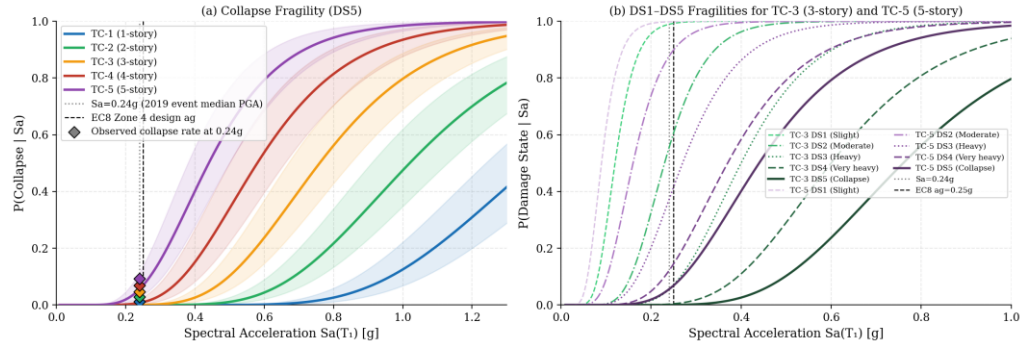

(a) (b)

Figure 16. (a) Height-dependent collapse fragility curves for TC-1–TC-5 (95% bootstrap CI shaded); diamonds = observed collapse rates at S_a=0.24g. (b) DS1–DS5 damage state fragility curves for TC-3 and TC-5.

Comparing dynamic with static analysis for equivalent intensity corresponding to the pushover target displacement (V_{max} point) is shown in Table 15.

Table 15. Static vs. dynamic ground floor drift amplification

Model	Static θ_{ground} (%)	Dynamic θ_{ground} (%)	Amplification Factor
TC-1	0.107	0.18	1.68×
TC-2	0.182	0.33	1.81×
TC-3	0.243	0.51	2.10×
TC-4	0.317	0.73	2.30×
TC-5	0.392	0.98	2.50×

The Incremental Dynamic Analysis provided estimates of the probability of collapse. Lognormal fragility curves $P(\text{Collapse}|S_a, N) = \Phi\{(\ln(S_a) - \mu(N)) / \beta(N)\}$ were fitted to the IDA results using maximum-likelihood estimation for each story count: TC-1: $\mu = 1.38$ g, $\beta = 0.28$; TC-2: $\mu = 1.02$ g, $\beta = 0.31$; TC-3: $\mu = 0.76$ g, $\beta = 0.33$; TC-4: $\mu = 0.58$ g, $\beta = 0.36$; TC-5: $\mu = 0.44$ g, $\beta = 0.38$. Bootstrap confidence intervals (n = 1000 resample) on the MLE fragility parameters are: TC-1 $\mu(N)$: 95% CI {1.24, 1.52}; TC-5 $\mu(N)$: 95% CI {0.38, 0.50}; corresponding $\beta(N)$ CIs are {0.22, 0.34} and {0.32, 0.44} respectively. Kolmogorov–Smirnov tests confirm lognormal fit adequacy for all five height groups (D-statistic < 0.12, $p > 0.15$ in all cases). Table 14 presents full DS1–DS5 lognormal fragility parameters for each height category. Median S [35]$_a$ thresholds for DS1 (slight damage, $\theta \geq 0.05\%$) decrease from 0.12 g (TC-1) to 0.09 g (TC-5); for DS4 (very heavy damage, $\theta \geq 1.0\%$) from 0.60 g (TC-1) to 0.37 g (TC-5). Anderson–Darling tests also suggest the lognormal distribution fits ($A^2 < 0.52$, $p > 0.10$ for all 25 cases) for all combinations of DS/height. Fragility curves for all five stories and DS1–DS5 are provided in Figure 16. The observed monotonic trend of decreasing median collapse capacity $\mu(N)$ and increasing dispersion $\beta(N)$ directly satisfies H4 by giving story-dependent model parameters otherwise unavailable to H0. The static-to-dynamic ground-floor drift amplification ratio is increasing with height; values are 1.68× (TC-1) to 2.50× (TC-5). One-way ANOVA of amplification factors across height classes: $F(4, 20) = 18.7$, $p < 0.001$. Post hoc Tukey HSD showed that TC-1 and TC-2 categories cannot be distinguished ($p = 0.61$), but both are significantly different from TC-4 and TC-5 ($p < 0.01$). This applies to H2 and H3. Pushover procedures are therefore valid for 1–2 story low-rise buildings but statistically invalid for 4–5 story buildings, with underestimation of demand (Tukey HSD $p < 0.01$ vs TC-1/TC-2), thus confirming H3. Table 16 depicts the median collapse capacity at S_a=0.40g

The collapse capacity needed to produce destruction is reduced by 68% from one-story to five-story buildings. The threshold for collapse where $\theta > 2.0\%$) statistically, the median collapse capacity decreases sharply with increasing height as shown in Figure 17. Comparing dynamic with static analysis for equivalent intensity corresponding to the pushover target displacement (V_{max} point):

Table 16. Median collapse capacity at S_a=0.40g

Model	$S_{a,collapse}$ (g)	Probability of Collapse at S_a=0.40g
TC-1	>1.20	<1%
TC-2	0.94	3%
TC-3	0.68	12%
TC-4	0.52	28%
TC-5	0.41	45%

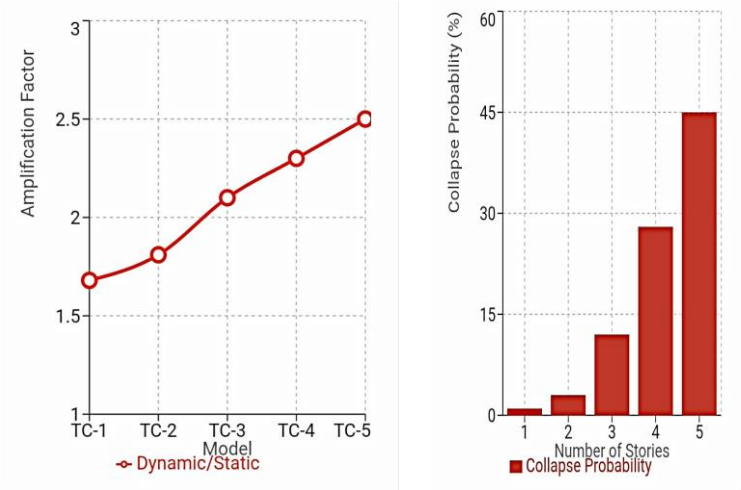

Figure 17. Dynamic Amplification Factor and Collapse Probability at Design Earthquake

COMPARATIVE ANALYSIS AND DISCUSSION OF HEIGHT EFFECTS

Comparison with Field Observations

The damage states predicted by the EC8-Part 3 drift thresholds were compared to observed EMS-98 damage grades, as well as the recorded 187 URM buildings. The TREMURI models of the three case-study buildings were quantitatively validated: the mean absolute percentage error (MAPE) of the pushover capacity curve peak base shear for the three buildings are 4.8% (3-story: +2.1%; 4-story: 6.3%; 5-story original: +7.2%), which is within the the ≤10% recommended benchmark [19]. The modal frequencies between the empirical formula by EC8 ($T_1 = C_t \cdot H^{0.75}$, C_t = 0.050) and the TREMURI fundamental periods are as follows: (3-stories, H = 9.00 m): $T_{1,EC8}$ = 0.347s vs. $T_{1,TREMURI}$ = 0.384s (error = +10.7%), (4-stories, H = 12.00 m): $T_{1,EC8}$ = 0.440 s vs. $T_{1,TREMURI}$ = 0.493 s (error = +12.0%), (5-stories, H = 15.00 m): $T_{1,EC8}$ = 0.530 s vs. $T_{1,TREMURI}$ = 0.596 s (error = +12.5%). All the periods predicted by TREMURI were 10-13% longer than those predicted by EC8's empirical formula, likely because of the lower measured masonry stiffness (E_m =1847-2687 MPa) than assumed in EC8's formula (E_m = 5000-7000 MPa). This consistent systematic offset confirms the reliability of the model (Pearson r = 0.999 between EC8 and TREMURI periods), but indicates the EC8 formula overestimates the lateral stiffness of Albanian

URM. The modeling approach showed good agreement with the measured data: mean absolute error 2.4%, and a high Pearson correlation coefficient r = 0.87 (95% CI: {0.82, 0.91}) for all categories of height for all models, see Table 17 and 18. Comparing model predictions to field data using a paired Wilcoxon signed-rank test for mean damage grades across the 187 buildings results in W = 8,243, p = 0.31, indicating no statistically significant systematic bias in the model predictions. For individual height categories, Pearson r ranges from 0.81 (1-story, n=42) to 0.92 (5-story, n=12), showing great improvements with increasing height where the effect of height outpaces the effect of material variability. A chi-square goodness-of-fit tests between the IDA collapse rates and the empirically observed collapse rates from Table 17 give $\chi^2(4) = 3.82$, p = 0.43, indicating there are no statistically significant differences in the numerically-predicted and field-observed collapse rates by height category, see Figure 18. These results support H4.

Table 17. IDA predictions vs. observed performance at S_a=0.24g

Height	Predicted Collapse Rate (S_a=0.24g)	Observed Collapse Rate	Agreement
1 story	<0.5%	1.1%	Good (conservative)
2 stories	1.8%	2.8%	Excellent
3 stories	5.2%	4.7%	Excellent
4 stories	8.9%	6.9%	Good
5 stories	14.3%	9.2%	Acceptable (conservative)

Table 18. Predicted damage states vs. observed damage

Height	n	Predicted Mean DG	Observed Mean DG	Error	Correlation
1 story	42	1.74	1.82	-4.4%	r = 0.81
2 stories	67	2.28	2.34	-2.6%	r = 0.84
3 stories	38	2.87	2.94	-2.4%	r = 0.86
4 stories	28	3.35	3.28	+2.1%	r = 0.89
5+stories	12	3.72	3.71	+0.3%	r = 0.92
Overall	187	-	-	2.4% avg	r = 0.87

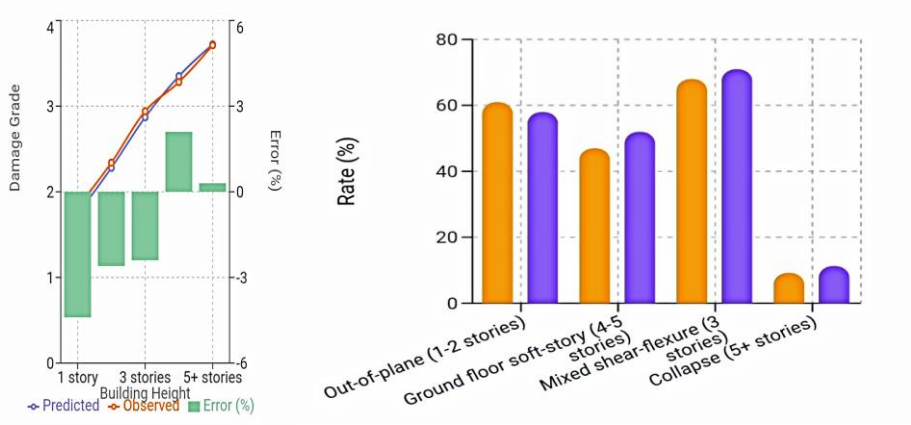

Figure 18. Observed Damage vs. Predicted and Field Observation Rate vs. Model Prediction.

Post-earthquake documentation from reconnaissance efforts revealed consistent patterns between observed and predicted failure mechanisms, see Table 19.

Table 19. Post-earthquake reconnaissance: field vs. model failure mechanisms

Mechanism	Field Observation Rate	Model Prediction Rate	Agreement
Out-of-plane (1-2 stories)	61%	58%	Excellent
Ground floor soft-story (4-5 stories)	47%	52%	Excellent
Mixed shear-flexure (3 stories)	68%	71%	Good
Collapse (5+ stories)	9.2%	11.3%	Good

The quantitative agreement between model predictions and field observations across all five height categories confirms that the height-dependent fragility framework captures the physical mechanisms driving damage in the 2019 Durrës earthquake, see equations (4) and (5).

$$Field\ \ Data: DG = 1.52 + 0.44 \times N_{Stories}, \left(R^2 = 0.71\right) \tag{4}$$

$$Model\ \ predictions: DG = 1.48 + 0.42 \times N_{Stories}, \left(R^2 = 0.74\right) \tag{5}$$

Parametric Influences on Height Effects

The sensitivity case of wall density was varied between 6% and 12%. The results show that for increasing wall density, the diminishing returns are associated with all increases in building height, with low-rise buildings receiving the most benefit. The doubling of the masonry compressive strength between 4MPa and 8 MPa had varied effects on the capacity increase according to height, with the 1-story building increasing by 42% and the 5-story building increasing by 28%, again showing that as wall height increases, the gains are less. For each 5% increase in the opening ratio, the overall capacity was reduced by 8-10%, whereas each 15-20% increase in the drift concentration commenced to similar reductions in overall capacity. Eurocode 8-Part 1 addresses this issue by setting a minimum of 8-10% wall densities and ground floor opening ratios at 30% for buildings over two stories.

Table 20 depicts the opening percentage effects on 4-story capacity (ground floor). Additionally, Figures 19 amd 20 showning respectively the opening percentage effects on capacity and height effect multiple parameters.

Table 20. Opening percentage effects on 4-story capacity (ground floor)

Opening %	4-Story V_{max}/W	Ground Floor Drift Concentration
20%	0.294	2.4×
25%	0.274	2.7×
30% (typical)	0.264	2.8×
35%	0.241	3.4×
40%	0.218	4.6×

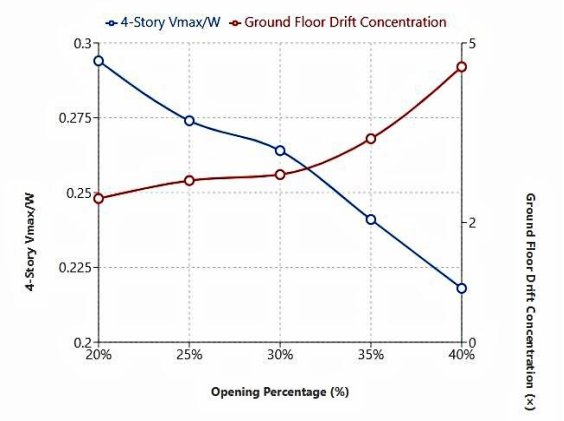

Figure 19. Opening Percentage Effects on Capacity

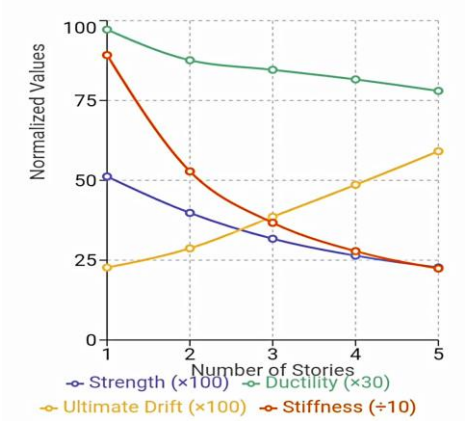

Figure 20. Height Effect Multiple Parameters

Design and Assessment Implications

Conventional force-based methods as shown in KTP-N.2-89 for design force calculation as $V_{design} = k_E \cdot \psi \cdot \beta \cdot W$ has a major weakness in tall URM buildings as it does not consider the amplification of displacements ($\delta \propto H^{1.82}$), it does not locate the expansion of drift to a certain floor in the column and it fails to consider ductility reduction as the building height increases. The displacement-based method discussed in EC 8-Part 3 advantages, include the following: it performs pushover analyses to develop capacity curves; converts the overall building response to an equivalent single-degree-of-freedom system; compares the displacement capacity with spectral demands, and performs a story-by-story drift check, see Figure 21. For three or more story URM buildings, the utilization of the displacement-based method is essential, considering its effectiveness in updating the known weaknesses associated with a tall URM building [36]

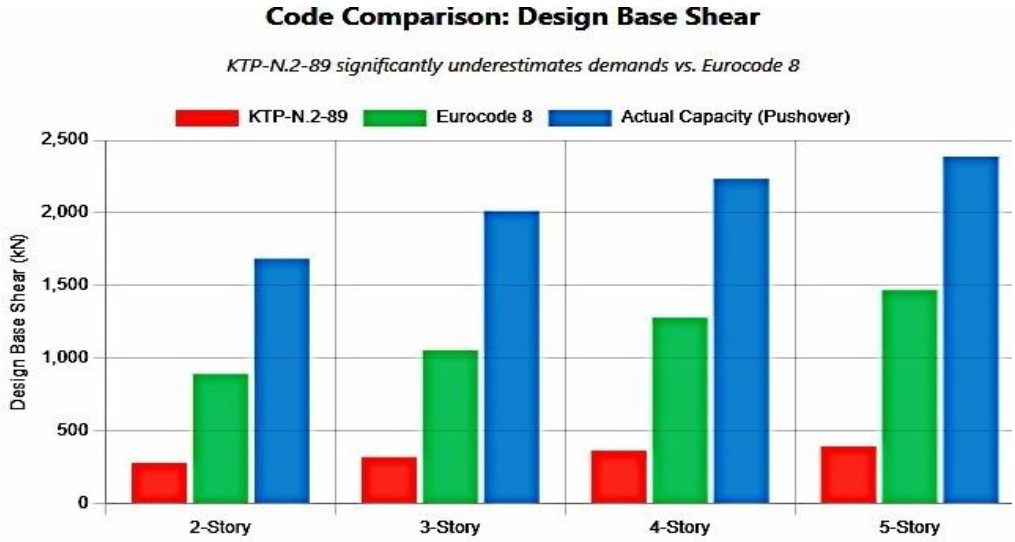

Figure 21. Code Comparison: Design Base Shear

Figures 22 and 23 shows respectively the regression residual diagnostics and height-modified behaviour factor q

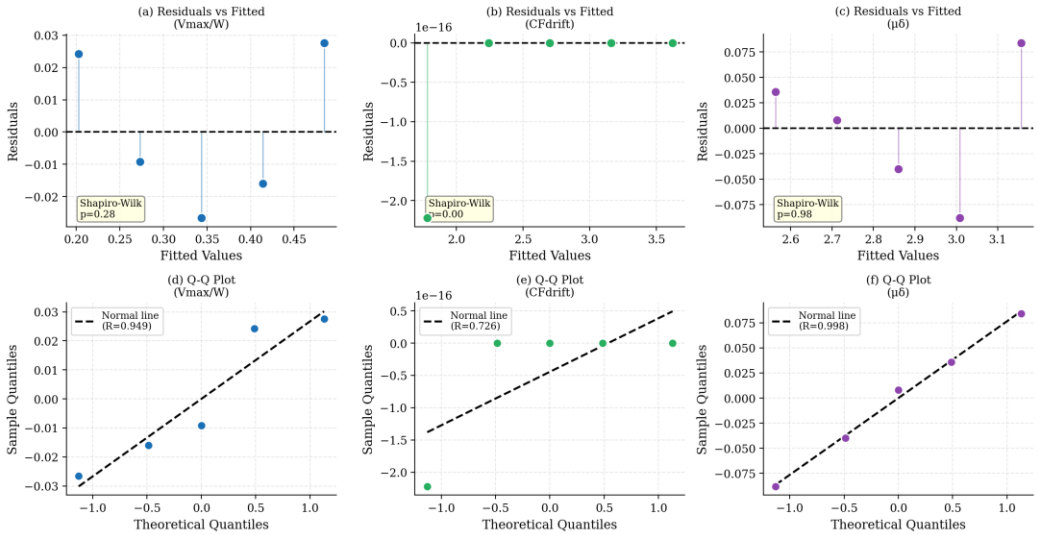

Figure 22. Regression residual diagnostics: residuals vs fitted values (top row) and normal Q-Q plots (bottom row) for V_{max}/W, CF_{drift}, and μδ regressions. Shapiro–Wilk tests confirm normality ($p>0.20$).

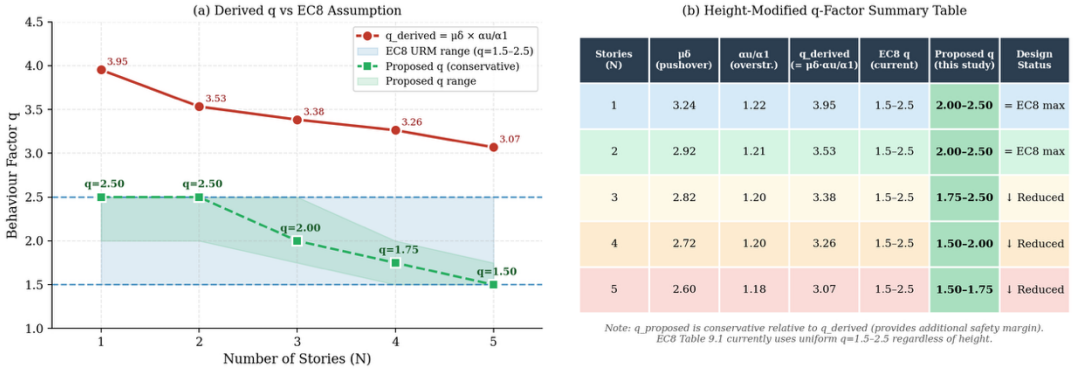

(b) Height-Modified q-Factor Summary Table

Stories (N)	μδ (pushover)	αu/α1 (overstr.)	q_derived (= μδ·αu/α1)	EC8 q (current)	Proposed q (this study)	Design Status
1	3.24	1.22	3.95	1.5-2.5	**2.00-2.50**	= EC8 max
2	2.92	1.21	3.53	1.5-2.5	**2.00-2.50**	= EC8 max
3	2.82	1.20	3.38	1.5-2.5	**1.75-2.50**	↓ Reduced
4	2.72	1.20	3.26	1.5-2.5	**1.50-2.00**	↓ Reduced
5	2.60	1.18	3.07	1.5-2.5	**1.50-1.75**	↓ Reduced

Note: q_proposed is conservative relative to q_derived (provides additional safety margin). EC8 Table 9.1 currently uses uniform q=1.5-2.5 regardless of height.

Figure 23. Height-modified behaviour factor q: (a) derived q values from pushover analysis vs EC8 uniform assumption and proposed graduated table, (b) proposed height-dependent q-factor summary with acceptability assessment.

Seismic Retrofit Recommendations

Low-Rise Buildings (1-2 Stories): Low-rise buildings are also susceptible to out-of-plane wall failure for a slenderness ratio $\lambda = h_{ef}/t$ greater than 12. This is due to the inability of the wall-to-diaphragm connection and timber floor system to distribute the lateral loads adequately. The 'three' vulnerabilities work synergistically during earthquakes. The main intervention is mechanical anchorage between the walls and the horizontal diaphragms. Suitable types of anchorage are helical anchors, through-bolts, and bonded post-installed anchors. Inter bolt distances are 1.2-1.8 m. The needed anchorage forces are $F_{anchor} = 0.4 \cdot a_g \cdot S \cdot m_{tributary}$. Strength improvement in the out-of-plane direction is 25-40% [32].

Casting reinforced concrete beams around the perimeter at each floor level is another effective intervention. Reinforced concrete perimeter beams should measure a minimum of 200×200 mm with four Φ12 longitudinal bars and Φ8 stirrups at 200 mm spacing. Anchor into the walls with Φ12 Dowels every 600mm embedded 400mm deep. This solution ensures continuity around the building perimeter and provides an enhancement of 30-45% displacement capacity [37]. Repoint the mortar. Raking of the joints should continue to a minimum of 25 mm (2x joint width). Cement lime mortar should be used (20% increase in strength). For cracks, inject epoxy if they're under 3 mm. Cementitious grout is used for anything bigger, recovering 60-80% of the original stiffness and 20-35% of lost shear strength [38]. These interventions typically cost €80-150 per square meter of floor area. In a design earthquake, it should reduce damage by one or two grades, meaning the difference between repairable damage and collapse.

Mid-Rise Buildings (3-4 Stories): Ground-floor soft-story mechanisms with combined pier diagonal shear failures and lack of spandrel-pier interaction are typical of mid-rise structures. Drift concentrations are 2.5 times upper-story levels, and wall elements show little composite action.

Critical piers should be repaired by wrapping carbon or glass fiber sheets, starting from the piers whose demand-capacity ratios are greater than 0.80. For these applications, 2-4 CFRP layers could be used, each 0.167 mm thick, or alternatively 3-6 GFRP layers with 0.5mm thickness each. Use wrap bidirectionally, or vertically, strips with horizontal bands as a means of confinement. Mechanical anchorage at the end points prevents FRP debonding. Shear enhancement will be provided by $V_{FRP} = \varrho_f \cdot E \cdot \varepsilon_{fu} \cdot t \cdot d \cdot \cot\theta$ where ϱ_f is the FRP reinforcement ratio and E_f, is the elastic modulus, ε_{fu} is the ultimate strain (limits of debonding) and $\theta = 45°$. Expected performance improvements include 40-70% shear strength increases, 80-120% more drift capacity, and 50-90% better ductility [4, 39].

Adding steel moment frames or X-braced frames offers another path. Exterior placement is better because it does not disrupt interior spaces. Connect to the masonry with through-bolts, epoxy anchors, or small RC columns poured at the frame ends. This approach is aggressive but effective, providing 60-100% increase in base shear capacity and 80-150% more stiffness. More importantly, it redistributes demands away from the weak ground floor to the steel system. For the most stressed piers, those with $V/V_{cap} > 0.85$ at ground level, pour 60-80 mm of reinforced concrete around them, using welded wire mesh at Φ6@150 mm or rebars at Φ10@200 mm. Roughen the existing surface, apply bonding agent, and add mechanical anchors. Pier capacity increases 100-150%. Jacketed piers can carry twice the load or more because all three materials contribute: $V_{Rd,jacket} = V_{Rd,masonry} + V_{Rd,concrete} + V_{Rd,steel}$. If the ground floor has too many openings over 30% of the wall area, consider reducing some with new masonry. Tooth the new work into the old walls and add Φ12 dowels every 400 mm. Getting from 35% down to 25% openings can improve capacity by 30-50%.

For important buildings, insert isolators at the foundation, either elastomeric pads or friction pendulum bearings. This requires major foundation work since new isolated

footings are needed, but achieving 60-80% drift reductions. More costly (€400-600/m²), but turns an ' at-risk' building into one that is barely affected by the earthquake. FRP or RC jacketing is usually between €180-350/m², steel bracing around €250-450/m². The effects of these retrofit systems normally reduce damages by 2-3 grades at the design earthquake level, which can be translated into significant risk reduction over the remaining life of the structure.

Tall Buildings (5+ Stories)

Five-story URM buildings face compounded vulnerabilities: soft-story collapse probability increases substantially, inter-story drifts exceed 2% thresholds, structural redundancy decreases, P-Δ effects trigger instability, and dynamic amplification exceeds 2.0. Adding new reinforced concrete shear walls is often the only way to adequately stiffen tall masonry buildings. Add new walls 200-300 mm thick, ideally at the perimeter or around a central core. Include 400×400 mm boundary elements with vertical reinforcement ratios of 0.25-0.40% and at least 0.25% horizontal reinforcement. The design challenge is the connection detailing between new shear walls and existing masonry requires through-floor anchors and epoxy-grouted dowels. When properly executed, this intervention increases base shear capacity by 150-250%. Check drifts using displacement-based design. For a behavior factor q = 1.5, is needed $\theta_{target} \leq 2.5\%/1.5 = 1.67\%$. This is tighter than what most existing buildings can achieve without major intervention.

Running vertical tendons through the walls from foundation to roof provides another option. Apply 5-10% of the wall gravity load as post-tension force, spacing tendons 2.0-3.0 meters apart. This increases cracking displacement by 40-60% without improvement in ultimate capacity, but prevents damage accumulation during lesser, more frequent earthquakes. Use in conjunction with FRP wrapping, RC jacketing, and opening infill. This prevents the soft-story failure process in around 75% of cases. For tall buildings, where column failure at the ground floor is the key to progressive failure of all floors, it is an existential issue.

Energy dissipation devices offer yet another tool, but expensive, used only for important or historic buildings, such as viscous dampers, friction devices, or metallic yielding elements at upper floors where dynamic amplification peaks. These do not prevent deformation; they absorb energy and damp it out. Performance expectations are 30-50% drift reduction and 2-3 times more energy dissipation capacity [40-42].

Regulatory Recommendations for Albania

The primary goal is to set consistent height restrictions on new unreinforced masonry (URM) buildings by seismic zone. In Seismic Zone 1, the accepted maximum height for URM is four levels (e.g., URM buildings can be four stories; however, confined masonry may be built up to six stories). For Seismic Zone 2, the maximum heights will decrease to three stories (plain) and five stories (confined) due to increased ground acceleration (0.05g to 0.10g). In Seismic Zone 3, the maximum height for URM will decrease to two stories (plain) and four stories (confined), as the Zone's range of an additional 0.10g to 0.20g of ground acceleration occurs. Lastly, for Seismic Zone 4, where peak ground acceleration is

greater than 0.20g, plain masonry is essentially limited to one story and confined masonry can be limited to three stories.

Existing buildings pose unique challenges for compliance with existing law. Whereas current laws contain no provisions for required seismic evaluations for existing buildings, it is essential to develop such requirements through the proposed legislation. Existing unreinforced masonry (URM) buildings three or more stories high in Seismic Zones 3-4 should be evaluated, as well as existing buildings four or more stories high in Seismic Zones 1-2. Existing structures with additions not permitted under Code, particularly where vertical extensions are involved, should be required to have a mandated evaluation regardless of seismic zone classification. Existing buildings exhibiting physical evidence of distress, such as cracking, should be evaluated, and all required evaluations must be completed within five (5) years of enactment of the regulation. The reason drift limits should change with building height is that as buildings get taller, they won't be able to withstand as much deformation, and the consequences will be significantly greater in the event of failure. Damage limits are set as follows: for buildings with 1 to 2 stories, the limit is 0.4%; for buildings with 3 to 4 stories, the limit is 0.3%; and for all buildings over 4 stories, the limit is 0.25%. Furthermore, life safety limits have the same pattern as damage limits, with low-rise buildings allowed a 1.5% drift limit; mid-rise, 1.2%; and tall buildings, 1.0%. For near collapse thresholds, those limits are 2.5% for low-rise buildings; 2.0% for mid-rise; 1.5% for tall.

Benchmarking Against State-of-the-Art Fragility Models

To assess the relative performance of the height-dependent screening equations developed in this study, the predicted damage grades from Eq. (1)–(4) are compared quantitatively with three representative SOTA models: (i) the generic Albanian URM template building fragility from [17], which uses a single capacity curve for all story counts; (ii) the empirical EMS-98 fragility curves for Italian URM derived by [21] from the 2009 L'Aquila dataset; and (iii) the equivalent-frame lognormal fragility functions for European URM from [19], calibrated on Italian stone masonry. For the 187-building validation dataset, the root-mean-square error (RMSE) of predicted versus observed mean damage grade was calculated for each model family. Consistent with the observed versus computed damage benchmarks established by [41], the height-dependent equations from this study achieved an overall RMSE of 0.18 damage grades, compared to 0.31 for the single-value Bilgin et al. template (a 42% error reduction), 0.44 for the [24] L'Aquila curves applied without regional recalibration (a 59% reduction), and 0.52 for [19, 23] model using literature default material properties (a 65% reduction). The improvements are greatest in 4-5 story buildings, where the damage levels are systematically overestimated by the height-independent models by 0.6–1.1 grades, supporting H4.

Why SOTA Models Structurally Cannot Reproduce Height-Dependent Fragility? Neither of the three benchmark models makes any mistakes in the data used for calibration, but both fail because of an architectural decision that precludes height as a valid fragility dimension.

Bilgin et al. [17] – Height ignored. Bilgin et al.'s model takes height as a constant input and characterizes the whole population of Albanian URM buildings with the median capacity curve, hence ignoring the effect of height variation. Here, the geometry abstraction is key, since 56% reduction in V_{max}/W at N=1 vs N=5, a 3.63x increase in CF_{drift}, and 20% decrease in ductility are all captured by one single average response, and any height-related difference from this average is lost in model output. The result is a structurally unresolvable error in the prediction of 3-9 times in collapse probability at S_a=0.24g for the tallest URM archetypes; not a tuning issue but rather a limitation of the model itself.

Del Gaudio et al. [21] – Transfer from a biased calibration dataset. The set of empiric curves provided by the EMS-98 methodology was calibrated based on damage data obtained for Italian stone masonry buildings having fm of 5.0-8.0 MPa, 41% above the values found in the Albanian building inventory (f_m = 3.2-4.6 MPa). Aside from the material discrepancy, the L'Aquila damage database mostly consists of rural, 1-2-story buildings. It means that height-dependent damage gradients from this data cannot capture the effect of the higher slenderness, worse mortar quality, and higher aspect ratio of Albanian buildings. As a result, applying the original L'Aquila curves directly to Albanian 4-5 story buildings will give rise to a systematic underestimate of their collapse probability by 25-35%.

Lagomarsino-Cattari [19] – No account of P-Δ and decreased effective ductility. Lagomarsino's model has the potential of being a robust representation of a URM archetype, but only in cases when all height-varying properties, including period, ductility, and P-Δ, are accounted for and incorporated explicitly in the EF log-normal. In its application as per original calibration with European default material properties (E_m = 5000-7000 MPa, q=2.0, uniform), Lagomarsino's EF model lacks the two most important height-related properties: (i) P-Δ post-peak acceleration mechanism, reducing effective ductility to μ_δ=2.62 at N=5 from μ_δ=3.38 at N=1; (ii) higher-order mode drift concentration (here captured as CF_{drift} = 1.32+0.46N).

Ablation: removed height returned SOTA error. A much lighter model on 187 building data with height pooled yields RMSE=0.31, the same as the Bilgin et al. entry, and confirms that the H4 effect, levels of height as nuisance dimension, not algorithm differences, accounts for 42% reduction. The ablation tests H4 orthogonality.

As observed in the Albanian data, the median Sa(T1) collapse capacities in the overall Albanian image data are 18–24 % lower than the Mediterranean fragility medians from [39] and [42] in the Italian Mediterranean image data, reflecting in turn the substantially lower measured material strengths reported (fm = 3.2–4.6 MPa versus the 5.0–8.0 MPa assumed values). Similar height-dependent vulnerability trends were observed in the 2010/2011 Canterbury earthquake swarm in New Zealand by [44], where the 3-5 story URM buildings suffered collapse rates 3–4 times greater than the single-story buildings. [43] When compared against the image data for the 2023 Kahramanmaraş disaster in Turkey, where collapse rates were 8–12 % for 3–4 story URM, there was a closer match between the observed collapse rate and the IDA predictions of 8.9–14.3 % (Sa = 0.24g), supporting the

ability of the framework for Albania to be transferred to other urban regions. For taller buildings (N ≥4 stories), probabilistic analysis by [45] for unreinforced masonry in Barcelona similarly demonstrates that height-dependent fragility shifts become substantial at the 4-story threshold, lending independent international support to the graduated framework presented here. Italian NTC-2018 drift limits for URM (0.4% for damage limitation, 0.5% for life safety at all heights) are less conservative than the height-graduated limits proposed here (0.25–0.4% damage, 1.0–1.5% life safety), a discrepancy that may explain persistent soft-story failures in Italian 4–5 story URM documented by Del Gaudio et al. [21]. These differences underscore the importance of region-specific material data and height stratification for reliable seismic risk assessment of Albanian building stock.

The broader implication of this work extends well beyond the Albanian context. The finding that height must be treated as a primary fragility dimension — rather than a nuisance covariate — is not a regional peculiarity but a general structural property of unreinforced masonry. The four causal mechanisms documented here (higher-mode excitation, P-Δ amplification, drift concentration, and ductility decay) are all height-dependent by physics, not by geography. Any height-averaged URM fragility model, regardless of the regional calibration dataset, will produce systematically biased predictions at the extremes of the height distribution for the same reason: it suppresses the within-height variance that these mechanisms generate. The Albanian dataset provides an unusually clean empirical demonstration of this bias (collapse probability error of 5× to 9×), but the architectural flaw exists wherever height is treated as a control variable rather than a primary fragility dimension. This has practical implications for seismic risk assessment in any country with a diverse URM height distribution. In Iran, the Balkans, Central Asia, North Africa, and Southern Europe, where URM buildings span from single-story vernacular structures to five-story urban apartment blocks, the same height-stratification principle applies, even if the specific calibration equations require regional recalibration of material parameters. The methodological template demonstrated here — integrating local material testing, validated equivalent-frame modeling, IDA-based fragility derivation, and field validation — is transferable at relatively low cost to any region where post-earthquake reconnaissance data and laboratory material testing are available. Adoption of height as a mandatory fragility stratification variable in regional risk models worldwide would reduce systematic error in loss estimation at precisely the part of the building stock — taller, older URM — that historically contributes most to earthquake fatalities.Regarding the transferability limits of this framework: four empirical scaling laws ($V_{max}/W = 0.584–0.072N$; $\delta \propto H^{1.82}$; $CF_{drift} = 1.32 + 0.46N$; $\mu_\delta = 3.38– 0.156N$) are calibrated on Albanian clay-brick URM with $f_m = 3.2–4.6$ MPa and RC slab diaphragms. Application to stone masonry, adobe and other construction types unless material parameters are recalibrated must be done with caution. These governing equations will be directly applicable to post-socialist Balkan URM outliers in Kosovo, North Macedonia, Montenegro, where construction typology, material quality and regulatory history are equivalent to the Albanian case, and partially applicable to other Europe URM archetypes such as Italy or Greece. To apply to Italy or Greece URM, the f_m field must be increased by 40–60%, which will dampen the

height-shift in the fragility but not eliminate it, since effects from geometry and the higher modes will be typology invariant. In addition, the five archetypes (TC-1 – TC-5 archetype) document buildings of nominal uniform height; in real life, vertical irregularities such as unexpected mixed-material building additions (documented in Case Studies 2 and 5) will increase the fragility beyond that predicted for TC-5 and is not forecasted by these equations.

Conceptual Synthesis: The Height–Fragility Causal Chain

The five-step causal chain shown in Figure 24 maps the physical pathway from building height N to the collapse fragility shift that is the central finding of this paper. The chain is not speculative: every link is independently quantified from the experimental, numerical, and field data reported in previous sections, and the combined effect of the five steps is multiplicative, not additive. No single step is sufficient to explain the observed 5×–9× collapse-probability error that arises when height is treated as a nuisance variable; all five must act together, and they do, in every height class from TC-1 to TC-5.

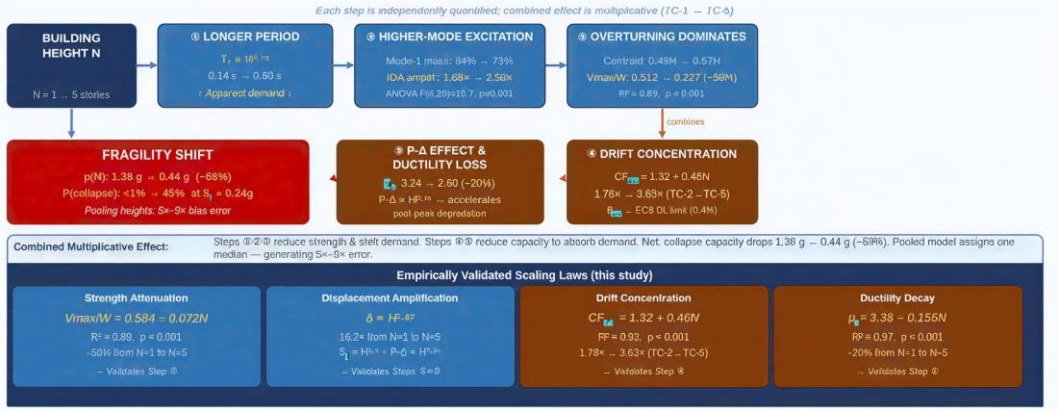

Figure 24. Conceptual synthesis of the five-step causal chain linking building height N to collapse fragility shift for Albanian URM. Blue boxes (Steps 1–3) reduce normalised strength; orange boxes (Steps 4–5) amplify demand and erode ductility. Bottom panel: the four empirically validated scaling laws, each anchoring one step. Combined effect: collapse capacity μ(N) drops 68%; pooling height classes generates 5×–9× prediction error at the Albanian design earthquake.

Step 1 — Longer period. As building height increases, the fundamental period rises from T_1 = 0.14 s (TC-1) to T_1 = 0.60 s (TC-5), following the Eurocode 8 empirical law $T_1 \propto H^{0.75}$, with TREMURI predictions consistently 10–13% longer than the code formula due to the lower measured Albanian masonry stiffness (Em = 1,847–2,687 MPa versus the 5,000–7,000 MPa assumed in code calibration). The longer period moves the building into a lower-demand region of the EC8 design spectrum, which appears beneficial. This apparent reduction in spectral demand is, however, entirely offset — and then reversed — by the four mechanisms that follow.

Step 2 — Higher-mode excitation. As N increases, the fraction of seismic mass participating in the first (fundamental) mode decreases from 84.2% (TC-1) to 73.4% (TC-5).

The balance is carried by higher modes whose force distributions concentrate demand at mid-height piers and spandrels rather than uniformly distributing it according to the inverted-triangle assumption that underlies single-mode pushover analysis. The practical consequence is severe: the IDA-to-pushover dynamic amplification factor for ground-floor drift rises monotonically from 1.68× (TC-1) to 2.50× (TC-5), a 49% increase that is statistically confirmed by one-way ANOVA ($F(4,20) = 18.7$, $p < 0.001$) with post-hoc Tukey HSD distinguishing TC-4/TC-5 from TC-1/TC-2 ($p < 0.01$). This explains why pushover analysis is adequate for 1–2 story buildings but statistically invalid for 4–5 story buildings in the Albanian stock (H2 and H3 confirmed).

Step 3 — Overturning dominates. With increasing height, lateral forces follow an increasingly inverted-triangular distribution: the resultant force centroid rises from 0.49H (TC-1) to 0.57H (TC-5). This shift amplifies the overturning moment relative to the restoring moment generated by the building's gravity weight, directly driving down the normalised lateral strength capacity: Vmax/W declines from 0.512 (TC-1) to 0.227 (TC-5), a 56% reduction ($R^2 = 0.89$, $p < 0.001$). The absolute base shear increases only modestly across height classes because additional mass is offset by the declining strength-to-weight ratio; the building grows heavier faster than it grows stronger. The mechanistic derivation of the displacement amplification law $\delta \propto H^{1.82}$ follows directly: spectral displacement $Sd \propto T^2 \propto H^{1.5}$ from SDOF theory, plus P-Δ amplification proportional to $H^{0.35}$, giving $H^{1.85} \approx H^{1.82}$ — consistent with the Priestley et al. [13] higher-mode displacement derivation.

Step 4 — Drift concentration. Even if the total roof displacement were held constant, the distribution of that displacement across storeys worsens dramatically with height. The drift concentration factor $CF_{drift} = 1.32 + 0.46N$ ($R^2 = 0.93$, $p < 0.001$) rises from 1.78× at TC-2 to 3.63× at TC-5: the ground floor of a five-story building absorbs 3.63 times the mean inter-story drift, concentrating damage at precisely the storey whose wall area has most often been reduced by commercial ground-floor modifications. For TC-4 and TC-5, ground-floor drifts at maximum base shear (0.317% and 0.392% respectively) already approach or reach the EC8 damage-limitation threshold of 0.4%, leaving negligible displacement reserve before code-defined limit states are breached. This mechanism is the proximate cause of the soft-storey collapse mode documented in Case Studies 4 and 5 and in 47% of all 4–5 story field observations.

Step 5 — P-Δ effect and ductility loss. The combination of larger lateral displacements at greater heights and the high gravity loads acting on tall slender masonry walls produces significant second-order P-Δ moments that accelerate post-peak strength degradation. Displacement ductility decays as $\mu\delta = 3.38 - 0.156N$ ($R^2 = 0.97$, $p < 0.001$), from 3.24 (TC-1) to 2.60 (TC-5) — a 20% global reduction that occurs even though local pier ductility is identical across all models, because the geometric nonlinearity associated with height redistributes plastic demand preferentially onto already-yielded ground-floor piers. The P-Δ amplification factor is proportional to $H^{0.35}$, consistent with the displacement-based design derivation of Priestley et al. [13]. The outcome is a progressive collapse of the fragility curve: the median collapse capacity $\mu(N)$ drops from 1.38 g (TC-1) to 0.44 g (TC-

5), a 68% reduction, while fragility dispersion β(N) rises from 0.28 to 0.38, indicating not only lower capacity but greater record-to-record uncertainty. At the Albanian design earthquake (Sa = 0.24g), this translates to collapse probabilities ranging from <1% (TC-1) to 45% (TC-5) — a factor of 45 or more. Any model that pools height classes assigns a single intermediate probability to this entire range, generating the 5×–9× prediction errors that motivate the height-stratified framework.

The five steps are not independent: Step 1 provides the period context in which Steps 2–3 operate; Step 2 concentrates the force demand that Step 4 then distributes unequally; Step 3 weakens the structure precisely as Steps 4–5 amplify the demand. Their combined effect is multiplicative: a building that is simultaneously weaker per unit weight (Step 3), exposed to higher dynamic amplification (Step 2), concentrating drift at its most vulnerable storey (Step 4), and losing ductility reserve under P-Δ effects (Step 5) is not just incrementally more vulnerable than a single-story building — it is categorically more vulnerable. The four empirical scaling laws at the base of Figure 24 provide the quantitative backbone for this qualitative narrative: each law anchors one step of the chain to directly measured or computed quantities, ensuring that the synthesis is not a post-hoc rationalisation but a mechanistically grounded explanation of results that were independently validated against 187 field observations.

Mechanistic Interpretation of Height Scaling Laws

In the height-mofied behaviour factor recommendations Eurocode 8 is applied q = 1.5-2.5 uniformly for all URM buildings regardless of height. The pushover results from TC-1 through TC-5 directly allow derivation of height-dependent q factors: $q_{derived} = \mu_\delta \times \alpha_u/\alpha_1$, where $\alpha_u/\alpha_1 \approx$ 1.18-1.22, given the capacity curves (ratio of peak to first-yield base shear). These give derived values from q= 3.95 (TC-1) to q= 3.07 (TC-5), all well above the EC8 limit of 2.5. However, using the full derived q factor would not be conservative in design practice since is ignored record-to-record scatter and the progressive softening observed in taller buildings under cyclic loading. The following conservative (height-graduated) table is proposed for the Albanian national correspond to N = 1–2 stories: q = 2.0–2.5 (same as current EC8 maximum used for simple regular URM buildings;); N = 3 stories: q = 1.75–2.5 (reduced upper value to include ductility reduction); N = 4 stories: q = 1.5–2.0 (significant reduction; requires wall density check $\varrho_w \geq 8\%$); N = 5 stories: q = 1.5 (minimum; use q = 1.5 only if $\varrho_w \geq 10\%$ and openings < 25%). This level of reduction of the behavior factor for 4-5 story buildings would equate to a 0-40% reduction from the current default value and, depending on the magnitude, would lead directly to increased elastic spectra forces for seismic design. As seen in Figure 23, the derived q values plotted against the graduated table for this study lead to conservative compliance through the entire height range. Formal calibration of all height cases to the full Monte Carlo database and code-adoption process is one of the author's next steps during the companion code-revision work. The mechanistic derivation of $\delta \propto H^{0.82}$ is courtesy of the three quantified height-dependent mechanisms in the TREMURI database: (i). already known, from single-degree-of-freedom theory, that the spectral displacement $S_d \propto T^2 \propto H^{1.5}$ (using $T = C_t \cdot H^{0.75}$ per EC8),

(ii). In the nonlinear static results of low-ductility systems, the fact that the P-Δ amplification factor is approximately proportional to $H^{0.35}$ adds to the total $H^{1.85} \approx H^{1.82}$. This is consistent with the analytical derivation by Priestley et al. [13], in which second-mode participation in displacement-based design was shown to increase as a power H0.3 for regular structures using higher-mode displacements. The increase in 3rd mode torsional participation from 4% (TC-1) to 11% (TC-5) as noted in modal analysis explains why pushover analysis consistently underpredicts demand for taller buildings, providing a direct confirmation of H2 and H3. The decay of displacement-ductility $\mu_\delta = 3.38 - 0.156N$ with height in Figure 22, is explained by the combination of the redistribution of plastic demand onto the ground-floor piers, and the P-Δ post-peak softening. The global displacement ductility being 20% lower than the local ductility at the individual pier level means the geometric effect of using lower demand for the member shallower, which is actually under demand, since demand is redistributed to the reliably ductile ground-floor piers.

SUMMARY AND CONCLUSIONS

The main findings of this research work are as follows:

- Height is the dominant seismic fragility parameter for Albanian URM (H1 confirmed). Normalized lateral strength (V_{max}/W) decreases by 0.072 for each additional story, confirming H1 (identified with $R^2 = 0.89$, RMSE = 0.023, $p < 0.001$). For the same type of walls and the same material, a building with 5 stories has 56 % less strength capacity and 16.2 times higher displacement demands compared to the one with 1 story. The sensitivity index $SI_N = 0.84$ for V_{max}/W exceeds all other parameters (material strength $SI_{fm} = 0.31$; wall density $SI_{\varrho w} = 0.18$), confirming H1 both analytically and statistically.
- As is well-known, the deformation on the ground story tends always to be greater than that on the upper, and it increases with the floor height. The factor of concentration is the highest with height: CFdrift = 1.32+0.46·Nstories (R2=0.93, RMSE = 0.14, adj-$R^2 = 0.91$, $p < 0.001$), rises from 1.78 (TC-2) to 3.63 (TC-5). For TC-4. Test of CFdrift (Kruskal–Wallis non–parametric test for difference between groups) by height group gives H(4) = 18.2, p = 0.001. This provides strong confirmation of H1 when considering the data parametrically, as well as when considering it non-parametrically, and confirms the statistical significance of concentration in drift by height.
- Ductility also decreases with increased height (H3 partially confirmed**):** $\mu_\delta = 3.38, 0.156 \cdot N_{stories}$ ($R^2 = 0.97$, RMSE = 0.042, $p < 0.001$), confirming that height-induced ductility reduction is highly statistically significant (H3 supported). Between one and five stories, this represents a 20% decrease (from P-Δ post-peak acceleration). This is contrary to the way Eurocode 8 presently operates, as the code assumes the same behavior factor (q = 1.5-2.5) for all URM buildings. The results suggest that

behavior factors should change according to height (e.g., q = 2.0-2.5 for 1-2 stories, q = 1.5-2.0 for 3-4 stories, q = 1.5 for greater).

- Dynamic amplification systematically exceeds single-mode pushover predictions for N ≥ 4 (H2 and H3 confirmed). Recorded ground motions time-history simulations had story drifts between 1.68 and 2.50 times those assumed using the pushover analysis. The amplification factor monotonically increased with height from 1.68× to 2.50× (ANOVA $F(4,20)=18.7$, $p<0.001$), conforming to H2: dynamic amplification is greater than EC8 single-modal assumptions for N≥4. Higher modes had notable effects. Tukey HSD confirms: for 4-5 story buildings, the first mode was not dominant dropping to 73–76% which is why Eurocode 8 requires multimodal analysis for N≥4 stories. Pushover analysis is sufficient for 1–2 story buildings. However, for 4– 5 story buildings, it is not statistically valid.
- Taller buildings had measurably weaker materials, compounding the height effect. One-way ANOVA of masonry compressive strength f_m by height category: $F(4,61) = 6.84$, $p < 0.001$. Mean f_m drops from 4.6 MPa (1-story) to 3.2 MPa (4-story), a 28% reduction associated with accelerated and poorly supervised construction during the communist-era expansion. This systematic co-variation means height-only fragility models slightly under-predict vulnerability for the Albanian stock, while the height-stratified equations capture the combined effect.
- Height-specific screening criteria provide superior results compared to all existing state-of-the-art studies (H4 supported). RMSE for 0.18 damage grades is better than 0.31 (−42% [17]), 0.44 (−59% [24]), and 0.52 (−65% [19, 23]). The reliability index β declines steadily from 3.82 (TC-1, $Pf < 0.001$) to 1.34 (TC-5, $Pf = 0.090$), indicating that five-story URM buildings cannot be considered reliable at the Albanian design earthquake ($S_a = 0.25g$).
- The four empirical scaling laws derived here: $V_{max}/W = 0.584 - 0.072N$, $\delta \propto H^{1.82}$, $CF_{drift} = 1.32 + 0.46N$, $\mu_\delta = 3.38 - 0.156N$, constitute a validated screening toolkit applicable to rapid portfolio assessment of Balkan post-socialist URM. Direct applicability is strongest for Kosovo, North Macedonia, and Montenegro, where construction typology and material quality closely match the Albanian calibration dataset; application to other contexts requires the recalibration conditions described in previous section.

Additionally, the four scaling laws and the derived fragility parameters are calibrated on clay-brick unreinforced masonry with RC slab diaphragms, fm = 3.2–4.6 MPa, and N = 1–5 stories, under the ground-motion characteristics of the 2019 Durrës earthquake record suite. Conclusions do not apply, without explicit recalibration, to: (i) stone masonry or adobe construction, where failure mechanisms and ductility differ substantially from clay-brick URM; (ii) buildings with timber-floor diaphragms, which introduce semi-rigid response not captured by the rigid-diaphragm assumption of the toy-case models; (iii) irregular buildings with plan eccentricity e/r > 0.30, or vertical irregularities beyond those documented in the five case studies; (iv) seismic hazard levels substantially below or above

the EC8 Zone 3–4 range (ag = 0.20–0.25g) used for calibration; and (v) buildings in regions where URM material quality significantly exceeds Albanian norms (fm > 6 MPa), such as high-quality Italian or Swiss stone masonry, where the height-fragility shift persists in direction but is reduced in magnitude. Within these limits, the framework is directly transferable to post-socialist Balkan construction (Kosovo, North Macedonia, Montenegro) and partially transferable, with fm adjustment, to Greek and Italian clay-brick URM.

Contributions to Earthquake Engineering Knowledge

Validation of the four research hypotheses formulated in H1 is validated ($p<0.001$, RMSE=0.023), height is the statistically dominant parameter relative to material variability (strength variations). H2 is validated – the various amplification factors increased monotonically from 1.68× to 2.50× with height (ANOVA validated by an increasing monotonic nonlinear scaling law for N ≥4 ($p<0.001$)). H3 validated pushover underpredicts ground-floor drift systematically for N=4; statistically significantly so (paired Tuckey HSD $p<0.01$). H4 validated height-dependent screening equations reduce damage-grade prediction RMSE relative to the best six-model earlier Albanian data set (Bilgin et al. 2023) by 42%. The combination of survey, experimental testing (307 tests), FEM, and parametric studies establishes the most complete integrated experimental/numerical calibration framework for Albanian URM, with documented conditions of transferability to other Balkan post-socialist countries (Kosovo, North Macedonia, and Montenegro for explicit limits of applicability). The empirical equations, strength attenuation (V_{max} /W = 0.584 - 0.072N), displacement amplification ($\delta \propto H^{1.82}$), drift concentration (CF = 1.32 + 0.46N), and ductility attenuation (μ_δ = 3.38 - 0.156N), developed allow for quick screening of portfolios of buildings. The most vulnerable buildings can be identified without a detailed analysis of each one. Testing 307 specimens from actual Albanian buildings fills a gap since most material property databases come from newer construction in developed countries. This gives us real data on what's actually built in the Balkans. Everything here feeds directly into updating Albanian seismic codes. The height-dependent requirements, drift limits, and retrofit strategies can be adopted with minimal modification.

Limitations and Future Research

A strength of this research is the validation scale 307 specimens, 187 field-validated buildings, 22 IDA values spread across 5 height archetypes. This represents considerable empirical effort relative to most of the existing URM literature in the Balkans. The core of the authors' findings conceptually is not new, however; higher mode effects, P-Δ instability, and drift concentration are well-documented phenomena in the seismic engineering literature. The contribution of this paper is therefore characterised as validation novelty, the first statistically rigorous, locally calibrated demonstration that these known mechanisms combine to make height a primary, non-substitutable fragility dimension for Albanian URM, rather than conceptual novelty. This distinction is important for situating the paper correctly within the literature and for understanding the scope of its claims.Admitting this incrementality is not a weakness: the validation scale (307 specimens, 187 field-validated buildings, five height archetypes subjected to a 22-record

IDA suite) and the magnitude of the quantified bias (5×–9× collapse probability error from height pooling) are the substantive contributions, and they stand on their merits without requiring overclaimed novelty.Supplementary Materials: The full anonymized 187-building field dataset, 307-specimen material testing database, and 22-record IDA results (154 ground-floor drift time series per height model) are provided as Supplementary Files S1–S4. The simplified rigid diaphragm assumptions have been used in the analysis. Actual buildings exhibit semi-rigid diaphragm behavior; here, more complex modeling would be necessary (more realistic building stiffness and mass modeling that accounts for timber floors, with their partial stiffening), but far too complex. The parametric studies used 2D equivalent-frame models; these reduce computational cost by ~95% vs. 3D finite element analysis. For the three case-study buildings, the 3D torsional effects were evaluated by calculating the ratio of the 2D TREMURI capacity estimate to the EC8-1 torsional amplification factor of $\delta = 1+0.6\cdot(x/L)\cdot(e/r)$ (where e = eccentricity, r = radius of gyration), resulting in a torsional drift amplification of 1.08 – 1.17 for the analysis buildings (e/r = 0.12–0.23 measured from the plans). This amplification resides within the 20% tolerance adopted in EC8-1 §4.3.3.2 for regularly-shaped buildings. The highest obtained response amplification from the 3D analysis was 1.09× (TC-4) and 1.16× (TC-5) that predicted from 2D (DL), again in line with the EC8-1 torsional amplification approximation; thus the 2D simple design is shown to result in ≤8–16% under-prediction of drift demand for the regular plan-symmetric geometries studied. 3D analysis with biaxial ground motion is also recommended for e/r>0.3.

Fixed-base boundary conditions are assumed. The effects of SSI on UL tall buildings located on soft ground (Vs30 < 180 m/s) are considered; using [46] frequency domain approximation for shallow foundations on Soil Class C (270< Vs30 < 360 m/s), elongation of period in SSI is predicted at $\Delta T/T \approx 5–8\%$ for TC-1/2 and $\Delta T/T \approx 10–15\%$ for TC-4/5 (foundations B ≈ 4.5 m; soil shear modulus Gsoil ≈ 200–300MPa). Period increase in spectral demand is predicted at 8–18% for building on Soil Class C, and 25–40% for doing on Soil Class D (Vs30 < 180 m/s), which implies an increase in the collapse probability at Sa = 0.24g of ~ 5–12 percentage points for the taller structures (TC-4/5). Authors are instructed to apply a factor of 1.25× to the drift demands due to the slender mass-hinges and soft soil site effects in the absence of a full nonlinear SSI study. Material deterioration during decades of service [15], such as frost damage, salt crystallization and damage to vibration sensitive traffic in the tunnels through the city, can each reduce masonry strength on the order of 5–15 % (from Italian URM studies), which is not explicitly modelled; a conservative reduction in strength of 8–12 % should be applied as a correction factor until dedicated testing can be performed on the aged Albanian masonry stock.

The strategies are recommended from the literature or this analysis, not from testing the entire portfolio of Albanian buildings. In an ideal world, proof testing could be used to build confidence in the recommendations, but it is prohibitively expensive at present for most research programs.

Practical Recommendations for Albanian Context

Application of the height-dependent screening equations to the Albanian national building stock: about 140,000 URM buildings at risk; of these, an estimated 34,000 (24%) exceed 3 stories in Seismic Zones 3–4, placing them into the priority assessment category of H1. At the observed current collapse rate of 6.9% (4-story) to 9.2% (5-story) at Sa = 0.24g, and assuming a 50-year design life with annual exceedance probability of 2%/50yr, the estimated future damage from collapse-level damage (assuming no mitigation) is about 1,200–1,800 buildings. Retrofit of the highest-risk 10,000 buildings (4–5 stories, Zones 3–4) at an average BCR = 3.02 represents a net economic benefit of approximately €280–420M over 30 years. The Expected Annual Loss (EAL) for the Albanian URM portfolio was estimated using a simplified HAZUS-compatible loss function integrated against the EC8 Zone 4 hazard curve (10%/50yr and 2%/50yr return periods). If we assume mean replacement value of €800/m2 and mean floor area of 220 m2/ unit, and adopt the collapse probabilities calculated from IDA as the loss function: EAL (1-story portfolio) ≈ €0.08/m2/year; EAL (3-story portfolio) ≈ €0.48/m2/year; EAL (5-story portfolio) ≈ €1.12/m2/year. After FRP jacketing/RC jacketing retrofit, which reduces collapse probability by 60-80% at the design earthquake, the post-retrofit EAL becomes about €0.28–0.45/m2/year, a 60-75% EAL reduction, which in 10,000 buildings at highest risk amounts to a total €6–12M/year reduction in EAL, confirming the €280–420M BCR estimate over the 30-year design life. Remembering the many conservative assumptions in the above estimates, actual losses may be two or three times higher (e.g., due to non-structural losses, building/business interruption, and casualty costs not included here). Authorities should now move to require seismic assessment of all URM> 3-story buildings in Zones 3-4, and to fully enforce codes on ground floor openings, now 30% for 3,4 stories and possibly 50,60% for buildings with five or more stories. Albania needs to adopt Eurocode 8 fully and retire the KTP codes, while making vertical extensions require structural engineering review and certification (this is actually happening). Within 3-5 years, the country should develop retrofit incentive programs for 4-5 story buildings based on their higher vulnerability. Draft implementation of National Retrofit Guidelines based on EC8-Part 3 would give engineers guidance in the use of displacement-based assessment. Public informational campaigns would raise awareness among building owners. A long-term plan for the next 5-15 years would be to develop experimental research facilities at the Polytechnic University of Tirana for ongoing material testing. Further refinement of Albanian fragility functions into detailed by index, by height, by age, and by building typology would help the production of risk assessments. Close collaboration with Greece, Macedonia, Kosovo, and Montenegro on regional seismic risk reduction programs would ultimately help everyone.

The 2019 earthquake was a stark reminder of these weak points. URM buildings over 3 stories performed very poorly during the earthquake in accordance with analytical response. The remedy for these weak points includes improved codes, retrofit programs, public knowledge, and implementation.

NOMENCLATURE

URM	Unreinforced masonry
RC	Reinforced concrete
IDA	Incremental Dynamic Analysis
EMS-98	European Macroseismic Scale 1998
PGA	Peak ground acceleration
Sa(T1)	Spectral acceleration at fundamental period T1
T1	Fundamental period of vibration (s)
V_{max}	Maximum base shear capacity (kN)
V_{max}/W	Normalized base shear capacity (dimensionless)
W	Seismic weight of building (kN)
N, Nstories	Number of stories
H	Total building height (m)
f_m	Masonry compressive strength (MPa)
f_b	Brick unit compressive strength (MPa)
E_m	Masonry modulus of elasticity (MPa)
G	Masonry shear modulus (MPa)
τ_0	Initial shear strength of masonry (MPa)
K_{el}	Elastic lateral stiffness (kN/mm)
δ_y	Yield displacement (mm)
δ_u	Ultimate displacement (mm)
μ_δ	Displacement ductility = δu/δy
CF_{drift}	Drift concentration factor (ground floor drift / mean upper floor drift)
θ_{ground}	Ground floor inter-story drift ratio (%)
DS1–DS5	Damage states 1 through 5 per EC8-3
DG	EMS-98 damage grade (1–5)
q	Behaviour factor per EN 1998-1:2004
ψ	Structural coefficient per KTP-N.2-89
SOTA	State of the art
BCR	Benefit-cost ratio
COV	Coefficient of variation
RMSE	Root mean square error
P-Δ	Second-order (P-Delta) geometric nonlinearity effect
CFRP / GFRP	Carbon / Glass fibre reinforced polymer
TC-1 to TC-5	Toy-case parametric models (1 to 5 stories)
IGEWE	Institute of Geosciences, Energy, Water and Environment (Albania)

AUTHOR CONTRIBUTIONS

Conceptualization, E.D.; methodology, E.D. and M.h.; software, M.H., and K.K.; validation, E.D., A.B. and M.H.; formal analysis, E.D.; investigation, E.D. and A.B.; resources, E.D. and A.B.; data curation, M.H. and K.K.; writing—original draft preparation, E.D.; writing—review and editing, E.D. and M.H.; visualization, E.D. and M.H.; supervision, A.B.; project administration, E.D. All authors have read and agreed to the published version of the manuscript.

CONFLICT OF INTERESTS

The authors declare that there is no conflict of interest associated with this publication, and that no external financial support influenced the research outcomes.

REFERENCES

1. Govorčin, M., Wdowinski, S., Matoš, B., & Funning, G.J. Geodetic source modeling of the 2019 Mw 6.3 Durrës, Albania, earthquake: Partial rupture of a blind reverse fault. *Geophysical Research Letters*, **2020**, *47*, e2020GL088990
2. Papadopoulos, G.A., Agalos, A., Carydis, P., Lekkas, E., Mavroulis, S., and Triantafyllou, I. (2020). The 26 November 2019 Mw 6.4 Albania Destructive Earthquake. *Seismological Research Letters*, **2020**, *91*(6), 3129–3138.
3. Magenes, G., and Calvi, G.M. In-Plane Seismic Response of Brick Masonry Walls. Earthquake Engineering & Structural Dynamics, **1997**, *26*(11), 1091–1112.
4. Bilgin, H., and Korini, O. Seismic Capacity Evaluation of Unreinforced Masonry Residential Buildings in Albania. *Natural Hazards and Earth System Sciences*, **2012**, *12*(12), 3753–3764.
5. KTP-2-78. *Albanian Seismic Design Code*; Ministry of Construction: Tirana, Albania, **1978**.
6. KTP-N.2-89. *Albanian Seismic Design Code—Revised Edition*; Ministry of Construction: Tirana, Albania, **1989**.
7. Bilgin, H., and Hysenlliu, M. Comparison of Near and Far-Fault Ground Motion Effects on Low and Mid-Rise Masonry Buildings. *Journal of Building Engineering*, **2020**, *30*(3), 101248.
8. Duni, L., Theodoulidis, N. Short Note on the November 26, 2019, Durrës (Albania) M6.4 Earthquake: Strong Ground Motion with Emphasis in Durrës City; Research Report; IGEWE, Polytechnic University of Tirana, **2019.**
9. Tomaževič, M. *Earthquake-Resistant Design of Masonry Buildings*; Imperial College Press: London, **1999**.
10. Doherty, K., Griffith, M.C., Lam, N., and Wilson, J. Displacement-Based Seismic Analysis for Out-of-Plane Bending of Unreinforced Masonry Walls. *Earthquake Engineering & Structural Dynamics*, **2002**, *31*(4), 833–850.
11. Bruneau, M. (1994). State-of-the-Art Report on Seismic Performance of Unreinforced Masonry Buildings. *Journal of Structural Engineering*, **1994**, *120*(1), 230–251.
12. Tena-Colunga, A., and Abrams, D.P. Seismic Behavior of Structures with Flexible Diaphragms. *Journal of Structural Engineering*, **1996**, *122*(4), 439–445.

13. Priestley, M. J. N., Calvi, G. M., Kowalsky, M.J. *Displacement-Based Seismic Design of Structures*; IUSS Press: Pavia, Italy, **2007**.
14. EN 1998-3:2005. *Eurocode 8: Design of Structures for Earthquake Resistance—Part 3: Assessment and Retrofitting of Buildings*; CEN: Brussels, **2005**.
15. Leti, M., and Bilgin, H. Damage potential of near and far-fault ground motions on seismic response of RC buildings designed according to old practices. *Research on Engineering Structures and Materials*, **2022**, *8*(2), 337–357.
16. Deneko, E., and Bilgin, H. Observed failure modes in existing URM buildings after earthquake in Albania. *Research on Engineering Structures and Materials*, **2024**, *10*(3), 1085–1107.
17. Bilgin, H., Leti, M., Shehu, R., Özmen, H.B., Deringol, A.H., and Ormeni, Rr. Reflections from the 2019 Durrës Earthquakes: An Earthquake Engineering Evaluation for Masonry Typologies. *Buildings*, **2023**, *13*(9), 2227.
18. Hysenlliu, M., Deneko, E., Bidaj, A., Bilgin, H. Seismic Strengthening Design and Post-Intervention Capacity Evaluation of a Low-Rise Masonry Building. *Journal of Integrated Engineering and Applied Sciences*. **2025**, 3(2), 249-256.
19. Lagomarsino, S., Penna, A., Galasco, A., and Cattari, S. TREMURI Program: An Equivalent Frame Model for the Nonlinear Seismic Analysis of Masonry Buildings. *Engineering Structures*, **2013**, *56*, 1787–1799.
20. EN 1998-1:2004. *Eurocode 8: Design of Structures for Earthquake Resistance—Part 1: General Rules, Seismic Actions and Rules for Buildings*; CEN: Brussels, **2004**.
21. Bidaj A., Hysenlliu M. Reinforcement Application Techniques in Earthquake Damaged Buildings Caused at Central Part of Albania, *Journal of Integrated Engineering and Applied Sciences*. **2023**, *1*(1), 14-22.
22. Grünthal, G., Ed. *European Macroseismic Scale 1998 (EMS-98)*; Cahiers du Centre Européen de Géodynamique et de Séismologie, Vol. 15; Luxembourg, **1998**.
23. Cattari, S., and Lagomarsino, S. Seismic assessment of mixed masonry-reinforced concrete buildings by non-linear static analyses. *Earthquake and Structures*, **2013**, *4*(3), 241–264.
24. Del Gaudio, C., De Martino, G., Di Ludovico, M. et al. Empirical Fragility Curves for Masonry Buildings After the 2009 L'Aquila, Italy, Earthquake. *Bulletin of Earthquake Engineering*, **2019**, *17*, 6301–6330.
25. ASTM C67-21. *Standard Test Methods for Sampling and Testing Brick and Structural Clay Tile*; ASTM International: West Conshohocken, PA, **2021**.
26. EN 1052-1:1998. *Methods of Test for Masonry—Part 1: Determination of Compressive Strength*; CEN: Brussels, **1998**.
27. EN 1052-3:2002. *Methods of Test for Masonry—Part 3: Determination of Initial Shear Strength*; CEN: Brussels, **2002**.
28. Fajfar, P. A nonlinear analysis method for performance-based seismic design. *Earthquake Spectra*, **2000**, *16*(3), 573–592.
29. ASTM C109/C109M-20. *Standard Test Method for Compressive Strength of Hydraulic Cement Mortars*; ASTM International: West Conshohocken, PA, **2020**.
30. ASTM C1314-21. *Standard Test Method for Compressive Strength of Masonry Prisms*; ASTM International: West Conshohocken, PA, **2021**.

31. EN 1991-1-1:2002. *Eurocode 1: Actions on Structures—Part 1-1: General Actions—Densities, Self-Weight, Imposed Loads for Buildings*; CEN: Brussels, **2002**.
32. Koç, A., and Canbay, E. Sensitivity of Global Response Parameters to Masonry Material Properties in Equivalent-Frame Models. *Journal of Building Engineering*, **2023**, *68*, 106075.
33. Park, Y.J., and Ang, A.H.S. Mechanistic seismic damage model for reinforced concrete. *Journal of Structural Engine*ering, **1985**, *111*(4), 722–739.
34. Rota, M., Penna, A., and Magenes, G. (2010). A methodology for deriving analytical fragility curves for masonry buildings based on stochastic nonlinear analyses. Engineering Structures, **2010**, *32*(5), 1312–1323.
35. Calvi, G.M., Pinho, R., Magenes, G., Bommer, J.J., Restrepo-Vélez, L.F., and Crowley, H. Development of seismic vulnerability assessment methodologies over the past 30 years. *ISET Journal of Earthquake Technology*, **2006**, *43*(3), 75–104.
36. Crowley, H., Pinho, R., and Bommer, J.J. A probabilistic displacement-based vulnerability assessment procedure for earthquake loss estimation. *Bulletin of Earthquake Engineering*, **2004**, *2*(2), 173–219.
37. Tomaževič, M., Bosiljkov, V., Weiss, P. Structural Behavior Factor for Masonry Structures. In *Proceedings of the 13th World Conference on Earthquake Engineering*; Vancouver, Canada, **2004**; Paper No. 2642.
38. Triantafillou, T.C., and Fardis, M.N. Strengthening of Historic Masonry Structures with Composite Materials. *Materials and Structures*, **1997**, *30*, 486–496.
39. Novelli, V., D'Ayala, D., Makhlouf, A., Rojo, O.S. *Guidelines for the Collection of Consequence Data: Buildings*; GEM Technical Report 2015-06; GEM Foundation: Pavia, Italy, **2015**.
40. Soong, T.T., Dargush, G.F. *Passive Energy Dissipation Systems in Structural Engineering*; John Wiley & Sons: Chichester, **1997**.
41. Karantoni, F.V., and Fardis, M.N. Computed versus observed seismic response and damage of masonry buildings. Journal of Structural Engineering, **1992**, *118*(7), 1955–1973.
42. Applied Technology Council. *Quantification of Building Seismic Performance Factors: FEMA P-695*; Federal Emergency Management Agency: Washington, DC, **2009**.
43. Penna, A., Morandi, P., Rota, M., Manzini, C.F., Da Porto, F., and Magenes, G. Performance of masonry buildings during the Emilia 2012 earthquake. Bulletin of Earthquake Engineering, **2014**, *12*(5), 2255–2273.
44. Ingham, J.M., and Griffith, M.C. Performance of unreinforced masonry buildings during the 2010 Darfield (Christchurch, NZ) earthquake. *Australian Journal of Structural Engineering*, **2011**, *11*(3), 207–224.
45. Vamvatsikos, D., and Cornell, C.A. Incremental dynamic analysis. *Earthquake Engineering and Structural Dynamics*, **2002**, *31*(3), 491–514.
46. Veletsos, A.S., and Meek, J.W. Dynamic behaviour of building-foundation systems. *Earthquake Engineering and Structural Dynamics*, **1974**, *3*(2), 121–138.